OPEN ACCESS Freely available online

PLOS ONE

Population Differentiation and Species Formation in the Deep Sea: The Potential Role of Environmental Gradients and Depth

Robert M. Jennings*, **Ron J. Etter, Lynn Ficarra**

Biology Department, University of Massachusetts Boston, Boston, Massachusetts, United States of America

Abstract

Ecological speciation probably plays a more prominent role in diversification than previously thought, particularly in marine ecosystems where dispersal potential is great and where few obvious barriers to gene flow exist. This may be especially true in the deep sea where allopatric speciation seems insufficient to account for the rich and largely endemic fauna. Ecologically driven population differentiation and speciation are likely to be most prevalent along environmental gradients, such as those attending changes in depth. We quantified patterns of genetic variation along a depth gradient (1600-3800m) in the western North Atlantic for a protobranch bivalve (*Nucula atacellana*) to test for population divergence. Multilocus analyses indicated a sharp discontinuity across a narrow depth range, with extremely low gene flow inferred between shallow and deep populations for thousands of generations. Phylogeographical discordance occurred between nuclear and mitochondrial loci as might be expected during the early stages of species formation. Because the geographic distance between divergent populations is small and no obvious dispersal barriers exist in this region, we suggest the divergence might reflect ecologically driven selection mediated by environmental correlates of the depth gradient. As inferred for numerous shallow-water species, environmental gradients that parallel changes in depth may play a key role in the genesis and adaptive radiation of the deep-water fauna.

Citation: Jennings RM, Etter RJ, Ficarra L (2013) Population Differentiation and Species Formation in the Deep Sea: The Potential Role of Environmental Gradients and Depth. PLoS ONE 8(10): e77594. doi:10.1371/journal.pone.0077594

Editor: Norman Johnson, University of Massachusetts, United States of America

Received July 8, 2013; **Accepted** September 12, 2013; **Published** October 1, 2013

Funding: This research was supported by NSF (nsf.gov) Grants OCE0726382 and OCE1130541. The funders had no role in study design, data collection and analysis, decision to publish, or preparation of the manuscript.

Competing interests: The authors have declared that no competing interests exist.

* E-mail: rob.jennings@umb.edu

Introduction

How species form is one of the most fundamental questions in evolutionary biology. Over the past two decades considerable progress has been made in identifying the scales, mechanisms, and driving forces of species formation in terrestrial and shallow-water ecosystems (e.g. [1-7]). However, little is known about these processes in the deep ocean, arguably the largest evolutionary realm on Earth with few obvious barriers to gene flow.

Geographic patterns of population genetic structure provide one of the primary lines of evidence for identifying the forces that might isolate gene pools. Marine organisms with pelagic dispersal were originally thought to disperse widely and show little population divergence [8], but recent empirical work has found that dispersal is much more constrained than typically inferred based on life histories (e.g. [2,9-11]). A number of mechanisms have been identified that might limit gene flow in marine ecosystems [3,12] including distance (isolation by distance – [13,14]), hydrographic features [15-17], nonrandom dispersal [18], gametic incompatibility systems [19-22], historical vicariance [23-27] and strong environmental gradients [28-33].

A growing body of evidence suggests that ecological speciation, defined as "the process by which barriers to gene flow evolve between populations as a result of ecologically based divergent selection between environments" [6], may be one of the key mechanisms of species formation in marine ecosystems (e.g. [7,34-37]). Population divergence is well known to occur along environmental gradients and may lead to the formation of new species [6,38]. Even weak selective gradients, as might occur with environmental gradients, can promote strong population divergence despite gene flow among continuously distributed populations [39]. Adaptation to local selective regimes can result in environment-phenotype mismatches such that larvae dispersing from their natal environment to a contrasting one would not survive to reproduce, effectively isolating populations [31,40]. Numerous

theoretical and empirical studies suggest selection along environmental gradients (e.g. temperature, moisture, altitude, salinity) promotes adaptation to different suites of abiotic and biotic conditions and ultimately may impede gene flow, leading to speciation (reviewed in [6,41,42]).

While considerable evidence exists for each of these mechanisms influencing population structure of shallow-water organisms, evidence of them operating in the deep sea is limited, apart from hydrothermal vents and other chemosynthetic ecosystems that have been more intensively studied (reviewed in [43,44]). Several interesting patterns have begun to emerge from the few phylogeographic studies of deep-sea organisms in non-chemosynthetic environments. The most distinctive is that isolation by depth appears to be much greater than isolation by distance [45-50]. For example, population divergence based on mitochondrial markers was much greater for protobranch bivalves separated by 3km of depth than 10,000 km of geographic distance [48,51]. Another interesting pattern is that population divergence appears to decrease with depth, suggesting that continental margins might be the primary site of adaptive radiation for deep-sea organisms [47,52-54]. Probably the most surprising result to emerge is that population divergence can occur on extremely small scales despite the lack of obvious oceanographic or topographic features that might impede gene flow [55,56]. The small-scale divergence is often associated with depth differences and likely reflects the strong environmental gradients that attend changes in depth. In some cases the divergence is sufficient to be suggestive of cryptic species [57-60].

These emerging phylogeographic patterns suggest that the environmental gradients paralleling changes in depth likely play an important role in the formation of new species in deep-water ecosystems [47]. Increasing depth is associated with changes in a wide variety of environmental variables including temperature, hydrostatic pressure, oxygen, hydrodynamics, habitat heterogeneity, and the nature and amount of food [61]. Singly or in combination, these environmental changes are thought to influence the bathymetric distribution of organisms and shape many of the major macroecological patterns involving alpha and beta diversity [62-64]. While their potential ecological roles have long been appreciated, their influence on evolutionary processes and dynamics remains poorly understood.

Here we document patterns of connectivity and quantify the scale and geography of population divergence in a common protobranch bivalve *Nucula atacellana* Schenck 1939 (formerly *Deminucula atacellana*) distributed across a depth gradient (1600-3800 m) in the western North Atlantic. Previous work using mtDNA (16S) identified strong genetic divergence among populations above and below 3000m [47,55]. These results were surprising because there were no obvious topographic or oceanographic features that might isolate populations from different depth regimes. Moreover, the distance separating these regions is less than 100 km, very likely within the dispersal window of *N. atacellana*'s demersal pelagic larvae. Several explanations might account for the divergence including idiosyncrasies of mtDNA (e.g. smaller effective population size, gender-biased dispersal), selection due to environmental changes associated with depth, or the presence of bathymetrically separated cryptic species. To better evaluate these alternative explanations, we quantify phylogeographic patterns using five loci, including both mitochondrial and nuclear markers. Recent work has stressed the importance of using multiple loci because mutational and coalescent stochasticity can lead to incongruent patterns among independent loci (e.g. [65-69]), and phylogeographic patterns often differ between nuclear and mitochondrial loci (reviewed in [24,70]). Our results indicate that *Nucula atacellana* has diverged across the depth gradient with very limited gene flow among bathyal and abyssal populations for more than 0.5 MY, possibly indicative of incipient speciation.

Methods

Ethics Statement

No specific permissions were required for collection of specimens, because they were collected in international waters below the continental shelf. Collection of specimens did not involve endangered or protected species.

Cruise and specimen collection

On a research cruise in 2008 on board the R/V *Endeavor*, specimens were collected along a transect closely following the Gay Head—Bermuda transect sampled by Hessler and Sanders [71]. At most stations two epibenthic sled tows were conducted; sediments were sieved and sorted live on board, in a chilled room (2°C) using chilled seawater to minimize stress to organisms. Following sorting, the remaining bulk samples were preserved in 95% ethanol and kept at –20°C. *Nucula atacellana* specimens sorted on board were either preserved by flash-freezing or by placing in 95% ethanol, and stored at –80°C. Additional specimens were sorted from the bulk samples after the cruise, also using chilled ethanol to slow DNA degradation. *N. atacellana* was collected at 9 of 20 stations (Figure 1, Table 1), across a depth range of 1600–3800m.

DNA extraction and locus amplification

Genomic DNA was extracted using the QIAamp Mini DNA Extraction Kit (Qiagen, Valencia, CA), using the standard animal tissue protocol with 2 sequential elutions of 100µL. PCR amplifications of mitochondrial COI and four noncoding nuclear loci (an actin intron (MAC), a calmodulin intron (CAL), and two noncoding anonymous fragments (DAC3 and DAC6)) were performed separately. Anonymous DNA markers were obtained by digestion of genomic DNA with the restriction enzyme AluI (NEB, Ipswich, MA), agarose gel selection of 1.0-1.5 kb fragments, cloning and sequencing; candidate markers were screened for polymorphism by sequencing a subset of the above specimens. Nuclear introns were selected based on a previous survey of introns in protobranch bivalves [72]. Standard PCR reaction mixtures were employed, and thermocycler conditions optimized for each locus (Table S1). In the few cases of poor amplification under these conditions, reamplification was performed with both a new negative control

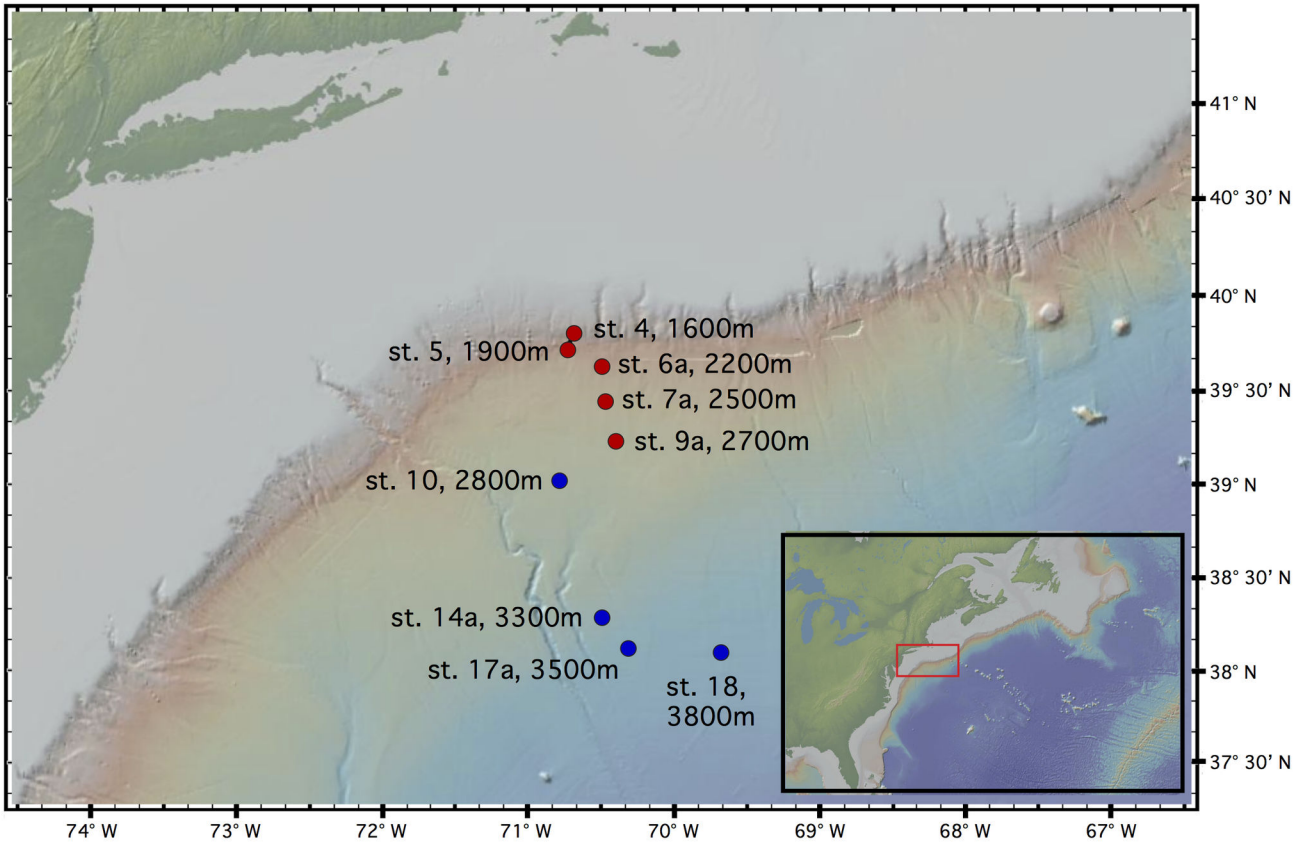

Figure 1. Map of sampled stations. The red box in the inset shows the location of the depth transect along the slope, rise, and abyssal plain of the Northwest Atlantic, with station names and depths indicated. Stations are color-coded according to a genetic separation between shallow (red) and deep (blue; see Results).

doi: 10.1371/journal.pone.0077594.g001

and reamplification of the original negative control, using nested primers where possible.

Sequencing, Heterozygote Detection, and Alignment

All successful amplifications produced single PCR bands as seen by gel electrophoresis, except for some individuals heterozygous at CAL for a 68bp indel that allowed separation of the two alleles in the gel. These alleles were gel purified and sequenced separately; all other single PCR bands were sequenced regardless of heterozygous status. Bi-directional sequencing was performed by Agencourt (a Beckman-Coulter company, Beverly, MA). The two reads for each individual were trimmed, aligned, and manually edited using Sequencher 5.0.1 (Gene Codes Corp., Ann Arbor, MI).

Individual base pairs were considered heterozygous if a clear double peak of near-equal height existed in both chromatograms, in the context of otherwise low or nonexistent background. Heterozygotes possessing alleles of different lengths (polymorphic indels) were ascertained by initially clear, single-peaked chromatograms that became almost-totally double-peaked (except for runs of a single nucleotide) while maintaining well-shaped peaks and regular spacing. The two juxtaposed sequences were deconvolved with the online program Indelligent [73]; each strand was deconvolved separately and the estimated alleles realigned to each other for

Table 1. Sampled station information, with coordinates, depths, and N collected.

Station	Depth (m)	Lat (°N)	Lon (°W)	N
4	1600	39.7807	70.7091	14
5	1900	39.7593	70.7132	12
6a	2200	39.6367	70.5033	30
7a	2500	39.4500	70.4667	12
9a	2700	39.2403	70.3993	8
Shallow Group				76
10	2800	39.0371	70.7812	6
14a	3300	38.2952	70.4940	2
17a	3500	38.1333	70.3167	5
18a	3800	38.1050	69.6933	6
Deep Group				19
Total				95

doi: 10.1371/journal.pone.0077594.t001

editing and quality control. Remaining heterozygous positions were phased using PHASE 2.1.1 [74,75], employing the Parent-Independent Mutation (PIM) model for sites containing indels or more than two bases. Any uncertain phases were estimated with a second run using haplotypes phased with certainty 1.00 as knowns (–k option). Sequences were aligned using the CLUSTAL algorithm [76] in BioEdit with default alignment parameters. For nuclear loci, both alleles of all individuals were included in the alignment. Final alignments were trimmed and checked manually.

Basic and Within-Locus Analyses

To ensure the noncoding status of nuclear loci, they were checked for the potential presence of coding sequences by BLAST searches against the GenBank nucleotide database, GenBank's ORF finder, the Gene Ontology database BLAST2GO [77], and AUGUSTUS [78]. Potential RNA secondary structure formation was assessed with Mfold [79].

Arlequin 3.5 [80] was used to compute basic indices and statistics for each locus separately: the number of haplotypes (Nhap), haplotypic diversity (H), and nucleotide diversity (π). Tajima's D (tested at α=0.05), and Fu's Fs (tested at α=0.02) were computed as basic tests of neutrality and demographic stability. Note that Arlequin excludes gapped positions (e.g. indels) when determining haplotypes; therefore, haplotype counts and diversity differ from other estimates. Based on initial indications of strong genetic separation at COI between a shallow group (stations 4–9a, 1600–2700m) and a deep group (stations 10–18/18a, 2800–3800m), indices and statistics were computed for each individual station with n≥3, for stations pooled among the shallow and deep group, and for all pooled individuals. For nuclear loci, deviations from Hardy-Weinberg equilibrium (HWE) were determined in Arlequin using default settings, computed among whole haplotypes. Within each locus, estimated recombination rates were determined between successive base pairs in PHASE [81,82], assuming a threshold of >5x background. Linkage disequilibrium (LD) among the nuclear loci was tested in Arlequin, using 1000 dememorization steps and 1,000,000 steps in the Markov chain.

As an additional test of selection, the McDonald-Kreitman test was performed by hand on COI, between the shallow and deep groups. Statistical significance was determined by computing the χ^2 statistic and p-value for the 2-by-2 contingency table of differences: Fixed vs. Variable and Synonymous vs. Nonsynonymous [83].

Population Clustering Analyses

Structure v2.3.4 [67] was used to determine the most likely number of populations (K) and to assign individuals to putative populations. The admixture model was employed, estimating separate α' s for each population, and setting λ=1 (the Dirichlet parameter for allele frequencies) for all populations. Allele frequencies among putative populations were modeled as uncorrelated (discussed in 84), and the chain was run with a burn-in of 100,000 steps followed by 500,000 steps. Twenty replicate runs per K were conducted for K=1 to K=10, and Structure Harvester [85] was used to choose K using the delta K criterion [86]. Because K=1 cannot be evaluated using delta K, the method of Pritchard et al. [67] for choosing K was also calculated. Output for the chosen K was analyzed in CLUMPP [87] using greedy heuristic searches with 5000 random permutations, and resulting admixture proportions were plotted using *distruct* [88].

Haplotype networks were constructed for individual loci in TCS [89], treating gaps as a 5th base (except for COI, where they represented missing data) and increasing the connection limit until all haplotypes were incorporated into a single network. For CAL, a large 68-bp indel (see Results) required two networks, one for the four "deletion haplotypes" and one for the remaining "insertion haplotypes".

The population clustering determined by Structure (see Results) was tested in Arlequin by AMOVA on all five loci, nesting individuals within stations, and stations within the shallow and deep groups. AMOVAs on multilocus and locus-by-locus pairwise differences were calculated with significance assessed from a null distribution of 1000 randomizations; multilocus pairwise Φ_{ST} and Φ'_{ST} values (Φ_{ST} standardized by its maximum attainable value [90]) were also calculated and tested for significance within this AMOVA framework. To test for isolation-by-distance (IBD) within each population, we regressed Slatkin's linearized Φ_{ST} against pairwise measures of (1) the log of geographic great-circle distance between stations and (2) the log of depth difference between stations, separately within the shallow and deep groups identified by Structure. Regression was performed via partial Mantel tests in Arlequin [91], removing the effect of depth on distance, and of distance on depth. Significance was assessed from a null distribution of 1000 random permutations.

Demographic and Population Genetic Analyses

The demographic history of populations was reconstructed in IM v.12.17.09 [92], using the populations determined by Structure and verified by AMOVA. The HKY mutation model was chosen for all loci, with a mutation rate for COI of 0.45%/(lineage·site·million-years), taken from an analysis of arcid bivalves by Marko [26]; mutation rates for nuclear loci were not specified. An Exponential Population Size Change Model was used because Extended Bayesian Skyline Plots (EBSP; see below and Results) indicated an exponentially growing shallow population. Separate analyses were conducted with and without COI. When COI was excluded, a mutation rate for CAL was used that had been estimated in BEAST calibrated with COI. Initial runs of 50,000 burn-in followed by 100,000 steps were performed to determine proper upper bounds for priors on population size (q), splitting time (t), and migration rates (m). Longer runs (>10^8) employed 10 Metropolis-coupled chains with a two-step increment model (as per the manual) and a burnin of 100,000, and were continued until all ESSs > 70. Three replicate runs with different starting seeds were performed to assess convergence. Parameters were converted to "demographic units" using a heuristic generation time of 10 years. The inferred demographic history was plotted using IMfig. An Extended Bayesian Skyline Plot (EBSP; [93]) was produced in BEAST 1.7.4 [94] as further analysis of demographic history. Convergence was assessed using Tracer 1.5, and demography plotted using scripts written by J. Heled

(https://code.google.com/p/beast-mcmc/downloads/detail?name=EBSP.zip&can=2&q=).

To determine the evolutionary history of populations and individuals, two applications of starBEAST [95] were used. In both applications, only the subset of fully sequenced individuals was used (n=74). Separate partitions were created for COI (single haplotype per individual) and each of the nuclear loci (both alleles included for all individuals), with substitution models, clock models, and locus trees unlinked across loci. The "SRD06" mutation model was used for COI, and each nuclear locus was given a GTR model with estimated equilibrium nucleotide frequencies and four categories of gamma-distributed rate variation. All loci were modeled with uncorrelated lognormally distributed clocks, setting the mean COI rate to 1.0 and estimating the others relative to COI. Starting trees were obtained by UPGMA, and a Yule prior was enforced with a piecewise linear population size and a constant root. Default priors were used for all parameters except for relative mutation rate priors for COI and clock mean rate priors, which were set to normal distributions with means and standard deviations of 1. Operators were tuned automatically, with weights adjusted per the BEAST manual. The MCMC chain was run for 10^7 steps; burnin was determined with Tracer 1.5 and consensus trees obtained with TreeAnnotator 1.7.4. In the first application, a "population tree" was created by assigning each individual to the population inferred with Structure. In the second application, a genealogy of individuals was created by assigning all nine sequences of an individual to that individual.

Results

Within-Locus Indices and Tests

Four nuclear loci and one mitochodrial locus were successfully sequenced from 95 individuals collected from 9 stations along a depth gradient from 1600-3800 m in the western North Atlantic (Table 2). Heterozygous indels were detected in all four nuclear loci: the 68bp indel in CAL was flanked by two indels of 4bp each, and the MAC intron contained six 1bp indels, one 2bp indel, and one 5bp indel. DAC3 contained a short run of TA repeats, and DAC6 contained 4 short indels (1bp, 1bp, 3bp, and 5bp). All sequences were deposited in GenBank (Accessions KC563091-KC563901, Table 2). No significant BLAST matches were found in the four nuclear loci, nor were ORFs or likely RNA secondary structures detected. Among all loci, DAC3 had the most haplotypes, followed by MAC, COI, CAL, and DAC6. Haplotype diversity was consistently very high; however, the deep group showed noticeably lower haplotype diversity at COI (Two-way ANOVA with locus and depth group as factors, $p<0.001$; Tukey's post-hoc comparison of deep COI vs. shallow COI $p<0.001$). Tests of Hardy-Weinberg equilibrium showed no departures from neutral expectations, and tests of LD showed no disequilibrium among the nuclear loci (Table 3). For recombination, one location (bp 11–12 in MAC) showed evidence of a recombination rate 11x above background, but variance in this estimation within the PHASE run was greater than the mean.

Simple tests of neutrality revealed a few significantly negative values for Tajima's D at several loci (Table 2), with departures from neutrality more common and negative at COI and DAC3, less so at MAC and CAL, and not detected at DAC6. The McDonald-Kreitman test for COI revealed a ratio of polymorphic nonsynonymous to synonymous sites (Pn/Ps) of 0.0482, and a ratio of fixed nonsynonymous to synonymous sites (Dn/Ds) of 0.0625; Pn/Ps< Dn/Ds implies that potential selection is negative. The Neutrality Index was 0.771 (NI, calculated as (Pn/Ps)/(Dn/Ds)), corresponding to a proportion of selected sites, α, of 1-NI=0.229. The 2-by-2 contingency table χ^2 statistic was 0.0513 ($p=0.821$), indicating that COI is not under selection.

Population Clustering Analyses

Structure runs tended to exhibit small variance at the highest and lowest Ks ($K\leq3$ and $K\geq8$), with larger variance at intermediate K (Figure 2A); however, significantly lower likelihood scores at intermediate Ks resulted in the clear choice of K=2 based on the Evanno criterion (Figure 2B); applying the Pritchard criterion resulted in K=3, with support for no separation (K=1) essentially zero. Although admixture proportions were relatively variable within the shallow group, shallow vs. deep individuals were generally ascribed to separate groups (red vs. blue respectively; Figure 2C). Structure analysis of just the nuclear loci produced slightly different admixture proportions, but resulted in a clear choice of K=2 by Evanno and Pritchard criteria (Figure 2 D-F), and again essentially zero support for K=1. Assignment proportions for this K=2 configuration indicated that 76 individuals belonged to the shallow group, and 19 to the deep group.

The differential admixture of individuals at mitochondrial vs. nuclear loci was apparent in haplotype networks (Figure S1 vs. S2-S5). While all networks showed high allelic diversity, haplotypes of deep individuals were separated more in COI than in nuclear networks.

The AMOVA confirmed the Structure (K=2) results, indicating significant divergence between shallow and deep populations for each locus independently and when all loci were analyzed together, with little divergence within populations (Table 4). The congruence between nuclear loci and COI indicated that the depth-related divergence occurred across all loci and was not exclusive to the mitochondrion. Across all five loci, Φ_{ST}' s were generally higher between shallow and deep pairs than among shallow pairs or among deep pairs (Table 5); the standardized Φ'_{ST} had the same pattern of significant pairwise values (not shown). Particularly among deep stations, significant Φ_{ST}' s likely reflect small sample sizes. The significant separation of shallow and deep lineages was highly supported in the starBEAST genealogy (posterior probability 0.99-1.00, Figure 3), with no nodal support for significant substructure within either group. Although strong divergence was detected between depth regimes, we found little spatial structure within (Table 5). Isolation by depth was not detected within the shallow or deep populations; isolation by distance was statistically significant in the shallow group, but did not remain significant when the effect of depth was removed (Table 6).

Table 2. Alignment length, basic statistics, and neutrality indices.

LOCUS: length (bp)	Station	N seq	Nhap	H	π	Tajima's D	Fu's Fs
COI: 651	4	14	14	1.0000	0.0391	**-1.8636**	-3.0226
	5	12	12	1.0000	0.0390	**-1.8096**	-2.1712
	6a	30	28	0.9931	0.0369	**-1.9209**	**-8.2027**
	7a	11	11	1.0000	0.0430	-1.1550	-1.5718
	9a	7	7	1.0000	0.1404	-1.0090	1.3799
	Shallow Group	74	66	0.9930	0.0483	**-2.2523**	**-24.0637**
	10	6	3	0.6000	0.0077	**-1.4725**	2.9600
	14a	2	1	NC	NC	NC	NC
	17a	5	2	0.4000	0.0006	-0.8165	0.0902
	18 and 18a	6	2	0.3333	0.0005	-0.9330	-0.0028
	Deep Group	19	3	0.5088	0.0065	0.4950	6.4760
	Total	93	69	0.9759	0.0537	-0.9854	**-15.8231**
GenBank Accessions:	KC563091-KC563183						
CAL: 213	4	14	12	0.8810	0.1637	-0.6471	9.9960
	5	12	14	0.9457	0.0937	-1.3462	1.8912
	6a	30	27	0.9328	0.1568	**-2.0539**	4.3031
	7a	12	20	0.9819	0.1155	-0.5346	-2.0350
	9a	7	8	0.9011	0.1598	-0.9671	6.3583
	Shallow Group	75	57	0.9389	0.1396	-1.3957	-0.7906
	10	6	8	0.9394	0.0162	-0.4816	-2.1856
	14a	2	4	NC	NC	NC	NC
	17a	5	7	0.9111	0.1715	-0.9910	4.2845
	18 and 18a	5	8	0.9556	0.0887	0.5574	1.0135
	Deep Group	18	17	0.9508	0.0883	-0.3933	2.3883
	Total	93	69	0.9484	0.1322	-1.397	-3.5017
GenBank Accessions:	KC563184-KC563369						
MAC: 254	4	12	15	0.9203	0.0464	1.5091	-0.8412
	5	12	5	0.6957	0.0480	1.9469	11.0681
	6a	29	25	0.8814	0.0464	1.3970	-1.6835
	7a	11	17	0.9784	0.0560	0.7653	-2.2385
	9a	8	13	0.9750	0.0672	1.2362	-0.9699
	Shallow Group	72	62	0.9079	0.0508	1.0397	**-20.1198**
	10	3	5	0.9333	0.0220	-0.1057	-0.2168
	14a	2	3	NC	NC	NC	NC
	17a	2	4	1.0000	0.0291	0.2791	-0.0653
	18 and 18a	5	8	0.9556	0.0229	1.0291	-1.6752
	Deep Group	12	20	0.9819	0.0195	0.2111	**-7.3103**
	Total	84	77	0.9315	0.0485	0.8064	**-24.0620**
GenBank Accessions:	KC563370-KC563537						
DAC3: 296	4	14	17	0.9286	0.0141	**-1.7403**	**-7.5118**
	5	12	15	0.8659	0.0102	-1.4193	**-8.5114**
	6a	30	25	0.9249	0.0136	**-1.8374**	**-11.6838**
	7a	12	20	0.9855	0.0187	-0.9744	**-12.4493**
	9a	6	9	0.9545	0.0219	-1.3440	-1.4768
	Shallow Group	74	66	0.9471	0.0221	**-2.2682**	**-25.5301**
	10	6	9	0.9545	0.0114	0.5887	**-3.6440**
	14a	2	3	NC	NC	NC	NC
	17a	4	6	0.9286	0.0114	-0.5409	-1.3732
	18 and 18a	5	6	0.8889	0.0078	0.3845	-1.5081
	Deep Group	17	17	0.9055	0.0095	-0.4450	**-9.4151**
	Total	91	81	0.9495	0.0154	**-2.2212**	**-25.4005**
GenBank Accessions:	KC563538-KC563719						
DAC6: 333	4	14	10	0.8942	0.0513	0.8095	6.8154
	5	12	6	0.7826	0.0329	1.2646	8.2304

Table 2 (continued).

LOCUS: length (bp)	Station	N seq	Nhap	H	π	Tajima's D	Fu's Fs
	6a	27	17	0.8917	0.0443	0.2571	3.7999
	7a	12	14	0.9239	0.0421	-0.3096	0.5763
	9a	8	10	0.9333	0.0220	-0.6046	-0.6332
	Shallow Group	73	33	0.9207	0.0416	0.2287	0.5957
	10	6	8	0.9091	0.0074	0.1794	**-3.295**
	14a	2	2	NC	NC	NC	NC
	17a	4	4	0.7857	0.0074	1.1762	0.5530
	18 and 18a	6	5	0.8485	0.0085	1.5085	0.5711
	Deep Group	18	11	0.8571	0.0087	-0.0554	-1.9937
	Total	91	38	0.9025	0.0368	-0.0060	-1.1553
GenBank Accessions:	KC563720-KC563901						

Nseq, number of individuals sequenced; Nhap, number of haplotypes detected; H, haplotype diversity; π, nucleotide diversity. Tajima's D values are bolded if significant at α=0.05 and Fu's Fs if significant at α=0.02.

doi: 10.1371/journal.pone.0077594.t002

Demographic History

Coalescent reconstruction of demographic history as estimated in IM using all 5 loci revealed an ancestral population that split approximately 95,000 generations in the past, resulting in largely independent shallow and deep populations along the sampled depth gradient (Table 7A, Figure 4). Although no good estimate exists for protobranch generation times, a conservative value of 10 years (an estimate within the range reported by Zardus [96]) translates to a split of 0.95 million years ago (MYA). The demographic estimates indicated an ancestral effective population size of ~412,000, a smaller deep population (N_e~121,000), and a much larger shallow population (N_e~3,998,000), comparable to the relative population sizes produced by the starBEAST population analysis (Figure 4, inset). Migration rates between populations per generation were extremely low (10^{-7} -10^{-8}) and asymmetric with greater dispersal from the shallow to the deep population. Translation of these estimates into demographic units indicates that, of the 4 million individuals in the shallow population, approximately 5 migrate to the deep population each generation. Results were qualitatively similar for the IM analyses excluding COI (Table 7B). Effective populations sizes were lower, the splitting time was more recent and migration rates were somewhat larger (10^{-6} -10^{-7}), with overall migration still extremely low. All three replicate IM runs for each analysis (with and without COI) produced very similar estimates with 95% HPD overlapping extensively for all parameters (not shown).

The EBSP analysis of shallow population history also showed a likely increase in the shallow population size from its ancestral size to a current N_e of 2 to 3 million, over approximately the last 1MY (Figure 5). Median population size of the deep group EBSP indicated population growth starting about 0.023 MYA (not shown), but the 95% highest posterior distribution (HPD) was quite large, including both zero growth and unrealistically high growth. The smaller sample size of the deep population appears to increase the error around demographic reconstruction.

Table 3. A, Test of Hardy-Weinberg equilibrium (HWE) using whole haplotypes at all loci; B, P-values for tests of linkage disequilibrium using whole haplotypes at the four nuclear loci.

A.

Sample	p-value
st. 4	0.7136
st. 5	1.0000
st. 6a	1.0000
st. 7a	0.7941
st. 9a	1.0000
Shallow group	0.9944
st. 10	1.0000
st. 14a	1.0000
st. 17a	1.0000
st. 18	0.1591
Deep group	0.8928

B.

	CAL	MAC	DAC3	DAC6
CAL	–	0.1660	0.4850	0.2790
MAC		–	0.5110	0.0550
DAC3			–	0.2990
DAC6				–

doi: 10.1371/journal.pone.0077594.t003

Discussion

A strong genetic break across a depth gradient

The most striking feature of the phylogeographic analysis of *N. atacellana* is a sharp genetic break at 2700m across just 100m depth and 40km horizontal distance. Although the divergence is most obvious for the mitochondrial locus with no shared haplotypes between shallow and deep populations (Figure S1), the nuclear loci all show significant population structure (Tables 4 and 5, Figures S2–S5) and all analytical results were qualitatively the same when COI was excluded.

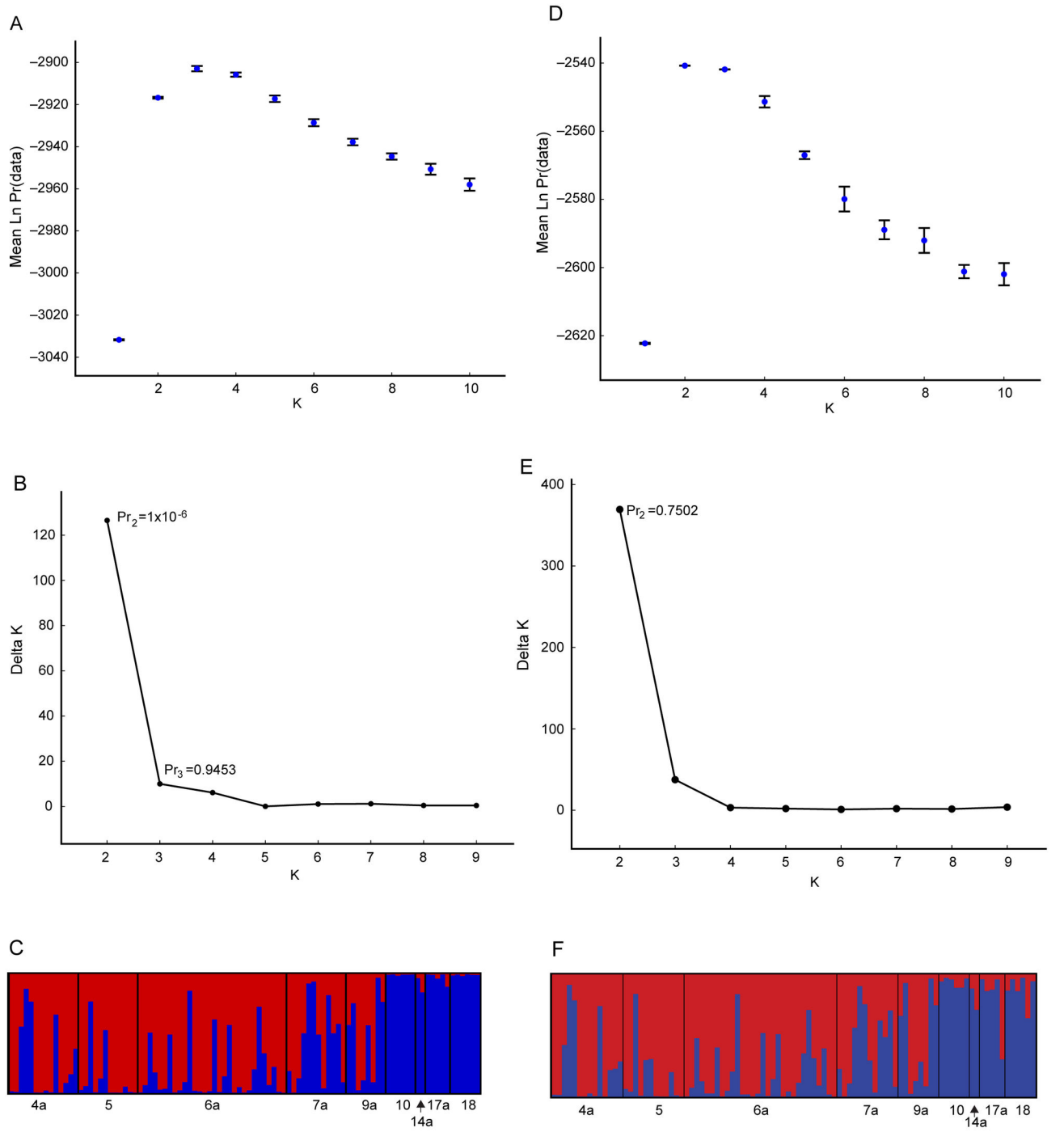

Figure 2. Structure analysis for all loci and just nuclear loci. A, Mean likelihood scores and standard deviations from 20 replicate runs at each K from Structure analysis of all 5 loci. B, Plot of Delta K model scores using the Evanno et al. method (2005); "Pr" indicates the probability for the best model (K=3) according to the method of Pritchard et al. (2000) and for the Evanno-selected K=2. C, Admixture proportions for the most likely grouping (K=2). D–F, the same analyses and measures for Structure analysis on nuclear loci only.

doi: 10.1371/journal.pone.0077594.g002

The location of the break is quite similar to previous findings for *N. atacellana* [47,55], but more intense sampling narrowed the depth separation between shallow and deep populations to 100m. Within depth regimes (i.e. 1600-2700m, and

Table 4. AMOVA analyses within each locus and with all loci combined.

Source of Variation	Locus	d.f.	Sum of Squares	Variance Components	Percentage Variation	p-value
Among Groups	All	1	961.671	14.7033	27.84	**<0.001**
	Nuclear	1	136.104	1.7928	8.00	**0.0049**
	COI	1	422.688	13.4951	50.76	**0.0108**
	CAL	1	66.294	0.8490	5.79	**0.0411**
	MAC	1	30.801	0.4997	7.61	**0.0059**
	DAC3	1	34.748	0.5635	21.01	**0.0049**
	DAC6	1	51.847	0.7614	11.53	**0.0098**
Among Populations,	All	7	484.910	0.3851	0.73	**<0.001**
Within Groups	Nuclear	7	185.100	-0.1622	-0.72	0.3275
	COI	7	105.061	0.2177	0.82	**0.0362**
	CAL	7	116.034	-0.0996	-0.68	0.4379
	MAC	7	74.205	0.0546	0.83	0.1075
	DAC3	7	27.019	0.0638	2.38	**0.0078**
	DAC6	7	49.323	-0.1866	-2.83	0.5298
Among Individuals,	All	86	5289.156	23.7825	45.04	**0.0327**
Within Populations	Nuclear	86	2555.643	8.9452	39.93	**<0.001**
	COI	84	1081.455	12.8745	48.42	**<0.001**
	CAL	84	1557.043	4.6176	31.48	**<0.001**
	MAC	75	722.232	3.6214	55.18	**<0.001**
	DAC3	82	216.315	0.5827	21.72	**<0.001**
	DAC6	82	876.825	4.6624	70.59	**<0.001**
Within Individuals	All	95	1324.000	13.9368	26.39	**<0.001**
	Nuclear	95	1123.500	11.8263	52.79	**<0.001**
	COI	–	–	–	–	–
	CAL	93	865.000	9.3011	63.41	**<0.001**
	MAC	84	200.500	2.3869	36.37	**<0.001**
	DAC3	91	134.000	1.4725	54.89	**<0.001**
	DAC6	91	124.500	1.3681	20.71	**<0.001**
Total	All	189	8059.737	52.8077		
	Nuclear	189	4000.347	22.4021		
	COI	92	1609.204	26.5873		
	CAL	185	2604.371	14.6681		
	MAC	167	1027.738	6.5626		
	DAC3	181	412.082	2.6825		
	DAC6	181	1102.495	6.6053		

d.f., degrees of freedom. P-values are bolded if significant at α=0.05.

doi: 10.1371/journal.pone.0077594.t004

2800-3800m), very little genetic differentiation was detected using Structure, AMOVA, or a Mantel test for IBD. Multilocus coalescent modeling suggests that the depth divergence reflects a historical population split some 0.95 MYA, with extremely low gene flow across the break since its inception. When COI was excluded, Structure, AMOVA, and IM still detected divergence between shallow and deep populations; although the estimated splitting time was younger (0.55 MYA; Figure S6). Taken together, therefore, there is strong evidence from both nuclear and mitochondrial loci for a significant genetic break between populations in close proximity along the depth gradient, and little divergence within shallow and deep depth regimes.

Discordance between COI and nuclear loci

It is not surprising that mitochondrial COI exhibits stronger genetic divergence than the nuclear loci because its smaller effective population size should speed the effects of genetic drift and lineage sorting once gene flow is disrupted (e.g. [24,65,97]). Estimated mutation rates at our nuclear loci are on the same order of magnitude as that for COI, but these loci have not attained reciprocal monophyly. This pattern is expected to arise early in the process of speciation. Speciation, ongoing or recent, is often invoked in explaining discordance between nuclear and mitochondrial loci (e.g. [24,70,98-100]), and such evidence has been found recently in several marine taxa [52,54,58-60,101].

An alternative explanation for the stronger mitochondrial divergence is that either COI or another mitochondrial gene is under selection. Significantly negative neutrality indices (Tajima's D and Fu's Fs) were detected for some samples and can indicate purifying selection; however, these tests are highly sensitive to fluctuations in demographic parameters such as population size [102,103]. In particular, exponential population growth can cause negative neutrality indices, and indeed there is evidence for growth in *N. atacellana*, especially in the shallow population (Figure 5) where most of the significantly negative neutrality indices were detected. The McDonald-Kreitman test detected no selection on COI, but provides little insight into selection on other mitochondrial genes. Although we have no evidence of selection on COI, we cannot rule out the possibility that selection is operating on the mitochondrion and could account for the greater divergence at this locus (see [104,105]).

Significant fixed differences in COI are often ascribed to cryptic species, which are commonly revealed when morphologically identified species are analyzed genetically (e.g. [23,46,57,70,106,107]). In *N. atacellana* the four nuclear loci analyzed display high allelic diversity and some differentiation by depth; however, full sequences of the nuclear small ribosomal subunit (18S) and a 718 bp fragment of the large subunit (28S) were 100% identical among shallow and deep individuals (data not shown). Although not conclusive evidence, these results do suggest that populations have not been isolated long enough for divergence to accumulate in these more slowly evolving genes, indicating that populations of *N. atacellana* may be at a very early stage of species formation.

What is disrupting gene flow across mid-rise depths?

The distance between the shallow and deep groups (100m depth, 40km distance) is almost certainly within the dispersal window of *N. atacellana*, which has demersal pelagic larvae that likely spend days to weeks dispersing [96,108]. The amphi-Atlantic distribution of *N. atacellana* [109] and the lack of genetic divergence across the North Atlantic [48] suggest dispersal distances are probably quite large, as has been found

Table 5. Pairwise Φ_{ST} values among sampled populations.

A. Pairwise Φ_{ST}, all loci									
	st4	**st5**	**st6a**	**st7a**	**st9a**	**st10**	**st14a**	**st17a**	**st18**
st4	–								
st5	0.0284	–							
st6a	-0.0079	0.0307	–						
st7a	0.0319	0.0438	0.0216	–					
st9a	0.0808	0.1048	**0.0882**	0.0756	–				
st10	**0.3497**	**0.3620**	**0.3295**	**0.3239**	**0.3469**	–			
st14a	0.3394	**0.3784**	**0.3438**	**0.3259**	0.3132	**0.4807**	–		
st17a	**0.2524**	**0.3139**	**0.2593**	**0.2592**	**0.2471**	**0.1738**	0.4075	–	
st18	**0.3233**	**0.3705**	**0.3135**	**0.3243**	**0.3375**	**0.0807**	**0.5128**	-0.0233	–
B. Pairwise Φ_{ST}, nuclear loci									
	st4	st5	st6a	st7a	st9a	st10	st14a	st17a	st18
st4	–								
st5	0.0507	–							
st6a	-0.0164	0.0497	–						
st7a	0.0089	0.0009	0.0025	–					
st9a	-0.0022	0.0475	0.0013	0.0162	–				
st10	**0.1987**	0.1137	**0.1783**	**0.1300**	0.2232	–			
st14a	0.1522	0.1203	0.1449	0.0927	0.1938	**0.2352**	–		
st17a	-0.0112	0.0394	0.0105	0.0146	-0.0624	**0.1755**	0.1610	–	
st18	0.0891	0.0617	0.0797	0.0538	0.0737	**0.1027**	0.1577	-0.0318	–

Statistically significant values are in bold. Station numbers are listed by increasing depth with a line separating shallow stations (4–9a) from deep stations (10a–18).

doi: 10.1371/journal.pone.0077594.t005

in other deep-sea taxa [110,111]. If connectivity between depth regimes is not limited by distance, then either hydrographic forces or selection (presumably at unsampled mitochondrial or nuclear loci) might be precluding gene flow.

The Deep Western Boundary Current (DWBC) flows south/southwestward in the immediate vicinity and depth of our sampled region, underneath and counter to the Gulf Stream [112,113], providing a possible isolating force to populations on either side. However, while the mean flow of the DWBC is southwest, highly complex small-scale variation is pervasive and probably more important for understanding actual particle trajectories and dispersal of largely passive invertebrate larvae. Drogues released at depth at three-month intervals over three years revealed significant submesoscale coherent vortexes (SCVs), long-lived eddies propagating from the DWBC and departing from its time-averaged southward trajectory [114]. The DWBC also interacts with the Gulf Stream, creating complex, variable, and non-isobathic water movements that could transport larvae from one side of the DWBC to the other [113-115]. Lagrangian simulations of particle releases in the DWBC show high potential for mixing and transport in the sampled region [115], making it unlikely that the DWBC is an effective barrier to gene flow. It is possible that larvae transported in SCVs from relatively cooler abyssal depths into warmer rise/slope depths or vice-versa face environmental challenges (see below) reducing or eliminating population connectivity through phenotype-environment mismatches (*sensu* [6,31]). It is also probable that the DWBC has waxed and waned through time in response to shifting climate [116,117] and was much stronger at times over the last 0.98 MY (i.e. through the glacial/interglacial cycles of the Pleistocene), possibly initiating the observed split in *N. atacellana*.

The lack of a clear isolating barrier and the extremely small scale over which divergence occurs suggest that selection might play an important role. A number of environmental gradients parallel changes in depth including temperature, oxygen, salinity, POC-flux, pressure, sediment characteristics, flow regimes, and topographic complexity as well as a suite of faunal characteristics such as the diversity, composition and trophic complexity of sediment communities [61-63]. Any of these gradients, singly or in combination, might lead to divergence, and they are frequently invoked as mediating adaptation (e.g. [118-120]), delimiting bathymetric distributions [62,121], or fostering population divergence and speciation [47,53,63,122,123]. Even weak environmental gradients can initiate divergence [38], and smoothly varying gradients can create sharply divergent taxa with deep phylogenetic splits [39]. In fact, the greater divergence at mitochondrial genes is exactly what we might expect if depth-related selection on mitochondria limited gene flow between depth regimes.

Identifying the precise environmental forces that shape bathymetric patterns of genetic variation will require considerably more research, but the greater divergence in COI compared to the nuclear loci is consistent with depth-related selection on mitochondrial variants. Metabolic processes might be especially sensitive to various depth-related environmental gradients (e.g. temperature, pressure, oxygen, etc.) leading to selection for different mitochondrial variants along the depth gradient. If this selection was strong enough to impede gene

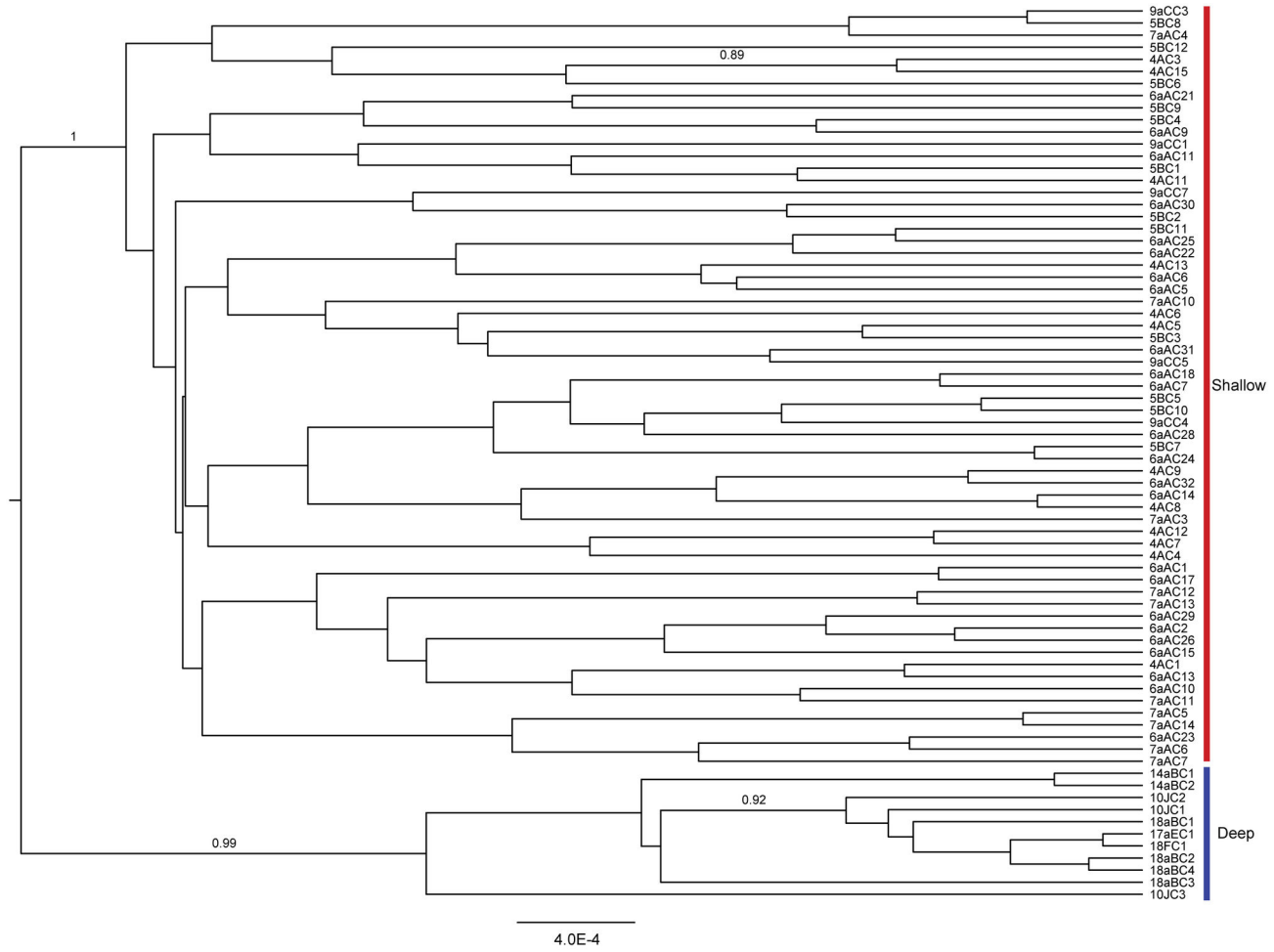

Figure 3. The starBEAST genealogy. Branch lengths are proportional to substitutions per site, combined across loci. Bayesian posterior clade probabilities are shown if >0.75, and population assignments are colored as in Figure 1.

doi: 10.1371/journal.pone.0077594.g003

flow by selecting against migrants from contrasting depths (e.g. immigrant inviability [40]) it could account for the discordance between mitochondrial and nuclear loci as well as the greater divergence of COI.

A consensus is emerging for both shallow and deep organisms that strong differences among populations from different depths may be caused by environmental gradients that parallel depth (e.g. [37,47,48,54,59,101,124-130]). For example, depth related divergence between populations of the coral *Eunicea flexuosa* appears to be related to strong environmental selection against ecophenotypes from contrasting depths that reduces gene flow and may ultimately lead to speciation [37]. Similar inferences were made for another shallow-water Caribbean coral *Favia fragum* [124] and for several deep-water corals [101,125,129,131]. In the coral *Seriatopora hystrix*, reciprocal transplants of depth-segregated, genetically distinct ecotypes implicated post-settlement selection against migrants from parts of the reef formation at different depths [123,132]. Even pelagic species exhibit depth-related divergence that likely reflects environmental gradients that parallel depth [54]. A rapidly growing body of evidence

Table 6. Mantel and partial Mantel tests of isolation-by-distance and -by-depth.

		Slatkin's Linearized Φst	
		r	p
Shallow Group	Distance	0.578	0.031
	Depth	0.334	0.141
	Distance (depth removed)	0.501	0.116
	Depth (distance removed)	-0.035	0.424
Deep Group	Distance	-0.320	0.795
	Depth	-0.229	0.729
	Distance (depth removed)	-0.429	0.781
	Depth (distance removed)	0.372	0.363

All spatial variables were converted to log(km).

doi: 10.1371/journal.pone.0077594.t006

Table 7. Demographic and historical parameter estimates from IM.

A. All loci				
Population Size	**Theta**	**95% HPD**	**Ne (x1000)**	**95% HPD**
Shallow	184.83	(109.01, 346.35)	3998.686	(2358.461, 7439.080)
Deep	5.60	(3.34, 9.09)	121.234	(72.333, 196.623)
Ancestral	19.07	(13.51, 26.61)	412.603	(292.388, 575.607)
Migration Rates	**m**	**95% HPD**	**Migration Rate**	**95% HPD**
Deep to Shallow	0.6370	(0.189, 1.389)	$7x10^{-8}$	($1x10^{-8}$, $1x10^{-7}$)
Shallow to Deep	0.0585	(0.011, 0.116)	$7x10^{-7}$	($2x10^{-7}$, $2x10^{-6}$)
Splitting Time	**Tau**		**Years (Millions)**	
	1.101	(0.759, 1.575)	0.953	(0.657, 1.363)
B. Nuclear loci				
Population Size	**Theta**	**95% HPD**	**Ne (x1000)**	**95% HPD**
Shallow	49.76	(37.73, 66.43)	318.319	(241.330, 424.919)
Deep	6.34	(3.66, 11.16)	40.567	(23.393, 71,363)
Ancestral	10.51	(6.90, 19.77)	67.217	(44.120, 126.439)
Migration Rates	**m**	**95% HPD**	**Migration Rate**	**95% HPD**
Deep to Shallow	0.7525	(0.278, 1.433)	$3x10^{-7}$	($1x10^{-7}$, $6x10^{-7}$)
Shallow to Deep	0.0735	(0.029, 0.155)	$3x10^{-6}$	($1x10^{-6}$, $6x10^{-6}$)
Splitting Time	**Tau**		**Years (Millions)**	
	2.186	(1.706, 3.602)	0.559	(0.438, 0.922)

The 95% highest posterior density (HPD) is given in parentheses. Ne, effective population size; Migration Rate, estimated migration rate per generation, forward in time from source to destination.

doi: 10.1371/journal.pone.0077594.t007

suggests selection along environmental gradients can lead to speciation despite continued dispersal (reviewed in [6]).

Consistent with depth and its attendant environmental gradients playing an important role in diversification of deep-sea species, numerous studies have documented strong bathymetric divergence suggestive of cryptic species [55,57-60]. In addition, divergence is consistently much greater among populations separated vertically than those separated horizontally [45-51]. For example, genetic divergence in the amphipod *Eurythenes gryllus* was much greater across a 3.6 km depth gradient than across 4000km at the same depth [45] or even between the Atlantic and Pacific [46]. Finally, we often find closely related congeners separated bathymetrically (e.g. [52,54,109,130,131,133,134]), precisely the pattern that would emerge if species formation was frequently mediated by depth-related environmental gradients. Depth is the most frequently observed habitat difference between sibling species [23].

The environmental gradients imposed by increasing depth in the oceans make an intriguing parallel to altitudinal gradients in terrestrial systems, with greater depth analogous to greater altitude. Numerous studies have documented gradients of lower genetic diversity with increased altitude in plants (reviewed in [135], also [136-138]) and animals (reviewed in [139], also [140-142]). While correlations in terrestrial systems are not always negative or linear, they are frequently accompanied by significant differentiation of highland and lowland clades [143-147], and often implicate the greater importance of vertical vs. horizontal distance. This was exactly the pattern documented in a widespread passerine bird in the Peruvian Andes, which was attributed to altitudinal shifts in selection on mitochondrial variants [148]. There is some evidence that, at least for animals, increased hypoxia at high altitude drives genetic differentiation and isolation-by-altitude [147-149], although adaptive changes in reproductive characteristics have also been found [150].

Another possible explanation for the depth divergence is that it formed in allopatry and the shallow and deep groups experienced secondary contact in the western North Atlantic, resulting in differential introgression of mitochondrial and nuclear genes. However, *N. atacellana* is widely distributed in the Atlantic, with virtually no divergence between the eastern and western North Atlantic and only modest divergence between the North and South Atlantic [48]. In addition, a similar depth divergence occurs within the Argentine basin but involves different haplotypes. Unfortunately, only formalin-fixed samples are available for the South Atlantic, restricting genetic analyses to mitochondrial loci. We cannot exclude the possibility that divergence was allopatric, but pan-Atlantic phylogeographic analyses indicate the greatest divergence is between shallow and deep groups in the western North Atlantic.

The deep ocean is a vast semi-continuous ecosystem that supports a highly diverse and largely endemic fauna. The evolutionary processes that gave rise to this distinctive fauna, the spatial and temporal scales over which they operate, and the geography and bathymetry of divergence are poorly understood. Given the limited ecological opportunity and the lack of obvious mechanisms that would allow population differentiation and speciation, it is unclear how new species form, especially at a rate sufficient to explain the high levels of diversity. Unraveling how and where evolution unfolds is critical for explaining biogeographic patterns of diversity [63], predicting how deep-sea ecosystems might respond to climate change [151-153], developing conservation and management strategies to mitigate the intense exploitation of deep-sea resources [64,154] and identifying appropriate locations and scales for MPAs [155,156]. Widespread and consistent divergence across depth gradients suggest depth and its concomitant environmental gradients may provide one of the primary mechanisms mediating population differentiation and speciation, especially below the continental shelves.

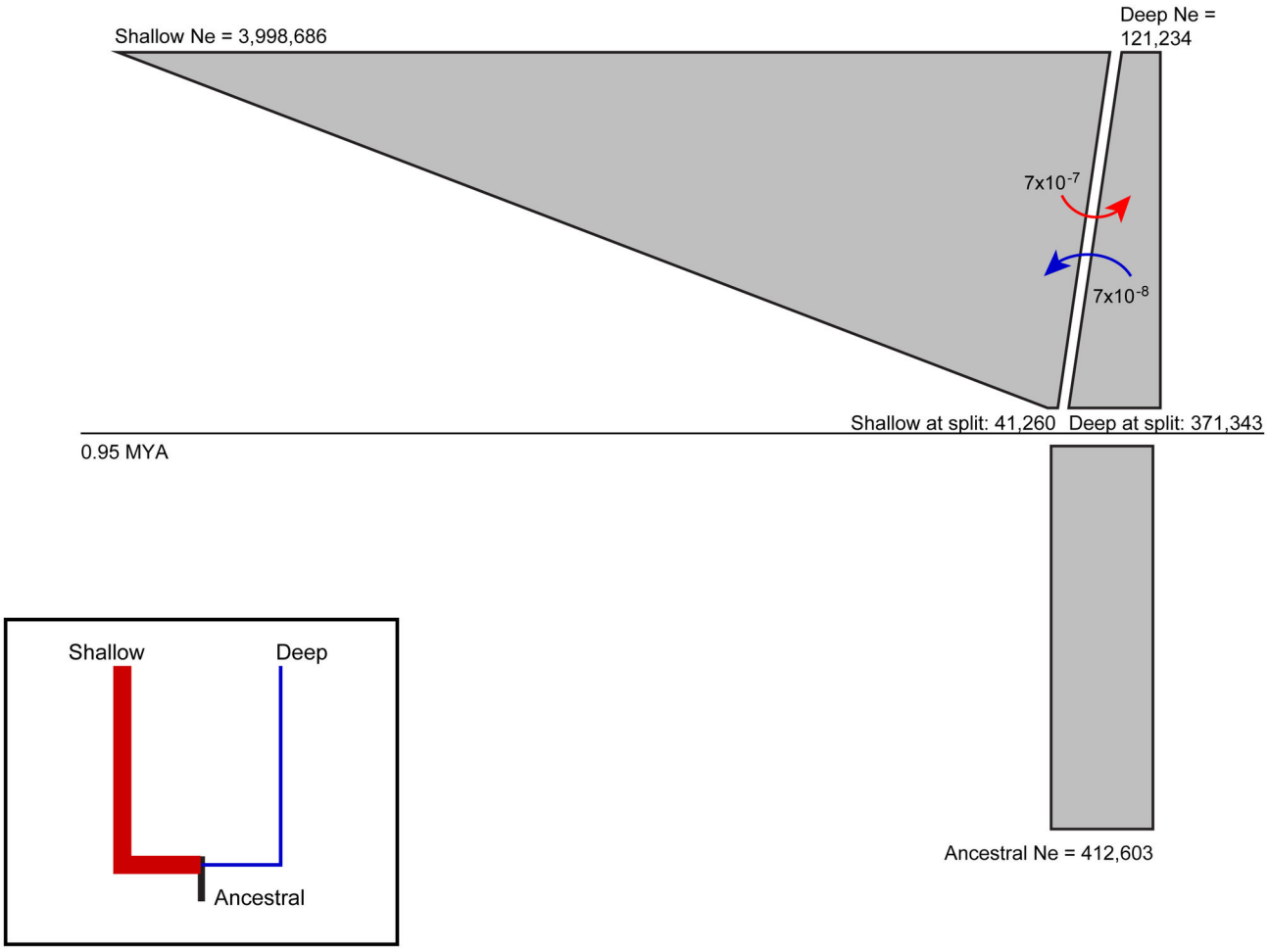

Figure 4. Population demographic history and migration estimates from IM for all loci. The gray box indicates the estimated effective population size (Ne) of the ancestral population. Estimated splitting time is indicated by the horizontal line. Descendant shallow and deep populations are represented above the line by polygons whose starting width is the estimated Ne just after the split and whose upper width is the estimated contemporary Ne. Curved dotted arrows represent estimated migration rates per generation, forward in time from source to destination. Demographic history estimation from starBEAST is shown in the inset, with branch thickness proportional to estimated population size. Coloring of shallow and deep is as in Figure 1.

doi: 10.1371/journal.pone.0077594.g004

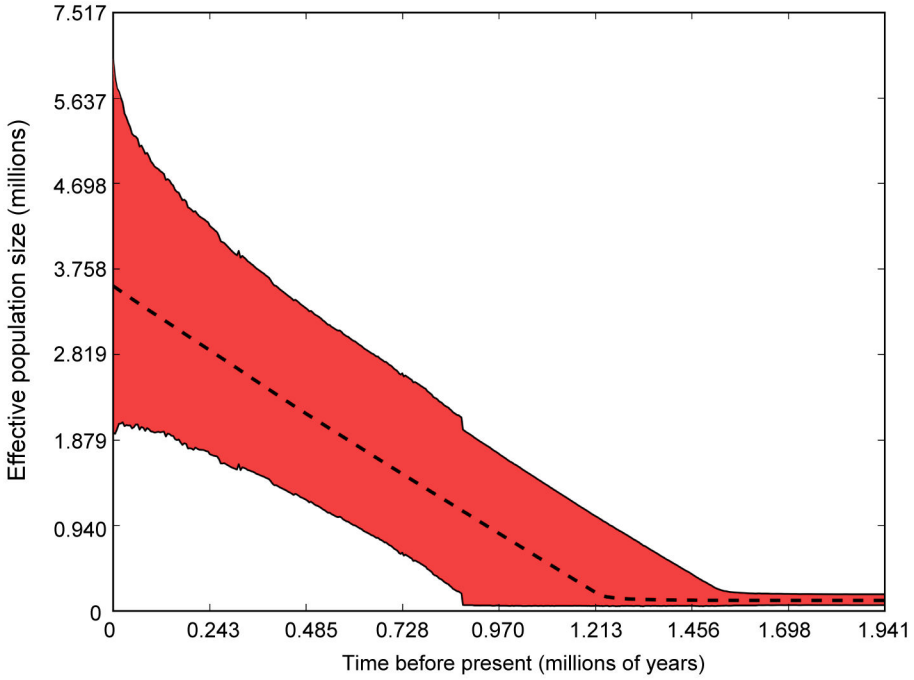

Figure 5. Extended Bayesian Skyline Plot of population size through time for the shallow population. Median (line) and 95% HPD (red shading) population size are shown.

doi: 10.1371/journal.pone.0077594.g005

Supporting Information

Figure S1. Haplotype network for COI. Circle size indicates number of individuals possessing that haplotype. Small circles represent unsampled haplotypes required to connect the network. Squares indicate the most likely ancestral haplotype. Haplotypes are shaded shallow and deep as in Figure 1.
(TIF)

Figure S2. Haplotype network for CAL. Haplotype shape, size, and coloring are as in Figure S1.
(TIF)

Figure S3. Haplotype network for MAC. Haplotype shape, size, and coloring are as in Figure S1.
(TIF)

Figure S4. Haplotype network for DAC3. Haplotype shape, size, and coloring are as in Figure S1.
(TIF)

Figure S5. Haplotype network for DAC6. Haplotype shape, size, and coloring are as in Figure S1.
(TIF)

Figure S6. Population demographic history and migration estimates from IM for nuclear loci. The gray box indicates the estimated effective population size (Ne) of the ancestral population. Estimated splitting time is indicated by the horizontal line. Descendant shallow and deep populations are represented above the line by polygons whose starting width is the estimated Ne just after the split and whose upper width is the estimated contemporary Ne. Curved dotted arrows represent estimated migration rates per generation, forward in time from source to destination. Coloring of shallow and deep is as in Figure 1.
(TIF)

Table S1. PCR reaction mixtures and thermocycler conditions for amplified loci. PCRs were performed in 50μL reactions consisting of 1X GoTaq Flexi buffer with loading dye (Promega, Madison, WI), 2.5mM $MgCl_2$, 2pmol dNTPs, 1.2pmol of each primer, 2μL genomic DNA, and 1 U of Taq polymerase (Promega). Conditions specific to each locus are given below; all protocols had an initial denaturation of 94°C for 3 min., 35 cycles of (denaturation at 94°C for 30 sec., annealing at the indicated temperature for 45 sec., extension at 72°C for 1 min), final extension at 72°C for 3 min., and a final hold at 4°C.
(DOC)

Acknowledgements

We thank the captain and crew of the R/V *Endeavor* and all participants of cruise EN447 for help in collecting and sorting samples. Elizabeth Boyle identified most of our protobranch specimens. Some analyses in this work were performed on the supercomputing facilities managed by the Research Computing Group at the University of Massachusetts Boston. We thank the editor and the anonymous reviewer for helpful and constructive comments on the manuscript.

Author Contributions

Conceived and designed the experiments: RJ RE. Performed the experiments: RJ LF. Analyzed the data: RJ RE LF. Contributed reagents/materials/analysis tools: RJ RE. Wrote the manuscript: RJ RE.

References

1. Coyne JA, Orr HA (2004) Speciation. 4 ed. Sunderland: Sinauer. 545pp.
2. Palumbi SR (2004) Marine reserves and ocean neighborhoods: The spatial scale of marine populations and their management. Annu Rev Environ Resour 29: 31–68. doi:10.1146/annurev.energy.29.062403.102254.
3. Hellberg ME (2009) Gene flow and isolation among populations of marine animals. Annu Rev Ecol Evol Syst 40: 291–310. doi:10.1146/annurev.ecolsys.110308.120223.
4. Sobel JM, Chen GF, Watt LR, Schemske DW (2010) The biology of speciation. Evolution 64: 295–315. doi:10.1111/j.1558-5646.2009.00877.x. PubMed: 19891628.
5. Butlin R, Debelle A, Kerth C, Snook RR, Beukeboom LW et al. (2012) What do we need to know about speciation? Trends Ecol Evol 27: 27–39. doi:10.1016/j.tree.2011.09.002. PubMed: 21978464.
6. Nosil P (2012) Ecological speciation. Oxford; New York: Oxford University Press. 304pp.
7. Bowen BW, Rocha LA, Toonen RJ, Karl SA, Laboratory TT (2013) The origins of tropical marine biodiversity. Trends Ecol Evol 28: 359–366. doi:10.1016/j.tree.2013.01.018. PubMed: 23453048.
8. Scheltema RS (1986) On dispersal and planktonic larvae of benthic invertebrates: An eclectic overview and summary of problems. Bull Mar Sci 39: 290–322.
9. Warner RR, Cowen RK (2002) Local retention of production in marine populations: Evidence, mechanisms, and consequences. Bull Mar Sci 70: 245–249.
10. Kinlan BP, Gaines SD (2003) Propagule dispersal in marine and terrestrial environments: A community perspective. Ecology 84: 2007. doi:10.1890/01-0622.
11. Levin LA (2006) Recent progress in understanding larval dispersal: new directions and digressions. Integr Comp Biol 46: 282–297. doi:10.1093/icb/024. PubMed: 21672742.
12. Palumbi SR (1994) Genetic divergence, reproductive isolation, and marine speciation. Annu Rev Ecol Syst 25: 547–572. doi:10.1146/annurev.ecolsys.25.1.547.
13. Hellberg ME (1996) Dependence of gene flow on geographic distance in two solitary corals with different larval dispersal capabilities. Evolution 50: 1167. doi:10.2307/2410657.
14. Bradbury IR, Bentzen P (2007) Non-linear genetic isolation by distance: implications for dispersal estimation in anadromous and marine fish populations. Mar Ecol Prog Ser 340: 245–257. doi:10.3354/meps340245.
15. Shulman MJ, Bermingham E (1995) Early life histories, ocean currents, and the population genetics of caribbean reef fishes. Evolution 49: 897–910. doi:10.2307/2410412.
16. Benzie JAH, Williams ST (1997) Genetic structure of giant clam (*Tridacna maxima*) populations in the West Pacific is not consistent with dispersal by present-day ocean currents. Evolution 51: 768–783. doi:10.2307/2411153.
17. Barber PH, Palumbi SR, Erdmann MV, Moosa MK (2002) Sharp genetic breaks among populations of *Haptosquilla pulchella* (Stomatopoda) indicate limits to larval transport: patterns, causes, and consequences. Mol Ecol 11: 659–674. doi:10.1046/j.1365-294X.2002.01468.x. PubMed: 11972755.

18. Hare MP, Guenther C, Fagan WF (2005) Nonrandom larval dispersal can steepen marine clines. Evolution 59: 2509–2517. Available: http://doi.wiley.com/10.1111/j.0014-3820.2005.tb00964.x. doi: 10.1554/05-150.1. PubMed: 16526499.
19. Metz EC, Palumbi SR (1996) Positive selection and sequence rearrangements generate extensive polymorphism in the gamete recognition protein bindin. Mol Biol Evol 13: 397–406. doi:10.1093/oxfordjournals.molbev.a025598. PubMed: 8587504.
20. Hellberg ME, Vacquier VD (1999) Rapid evolution of fertilization selectivity and lysin cDNA sequences in teguline gastropods. Mol Biol Evol 16: 839–848. doi:10.1093/oxfordjournals.molbev.a026168. PubMed: 10368961.
21. Palumbi SR (2009) Speciation and the evolution of gamete recognition genes: pattern and process. Heredity 102: 66–76. doi:10.1038/hdy.2008.104. PubMed: 19018273.
22. Lessios HA (2011) Speciation genes in free-spawning marine invertebrates. Integr Comp Biol 51: 456–465. doi:10.1093/icb/icr039. PubMed: 21700571.
23. Knowlton N (1993) Sibling species in the sea. Annu Rev Ecol Syst 24: 189–216. doi:10.1146/annurev.es.24.110193.001201.
24. Avise JC (2004) What is the field of biogeography, and where is it going? Taxon 53: 893–898. doi:10.2307/4135555.
25. Barber PH, Palumbi SR, Erdmann MV, Moosa MK (2000) A marine Wallace's line? Nature 406: 692–693. doi:10.1038/35021135. PubMed: 10963585.
26. Marko PB (2002) Fossil calibration of molecular clocks and the divergence times of geminate species pairs separated by the Isthmus of Panama. Mol Biol Evol 19: 2005–2021. doi:10.1093/oxfordjournals.molbev.a004024. PubMed: 12411609.
27. Lessios HA (2008) The great American schism: Divergence of marine organisms after the rise of the Central, American Isthmus. Annu Rev Ecol Evol Syst 39: 63–91. doi:10.1146/annurev.ecolsys.38.091206.095815.
28. Ganz HH, Burton RS (1995) Genetic differentiation and reproductive incompatibility among Baja California populations of the copepod *Tigriopus californicus*. Mar Biol 123: 821–827. doi:10.1007/bf00349126.
29. Dennis AB, Hellberg ME (2010) Ecological partitioning among parapatric cryptic species. Mol Ecol 19: 3206–3225. doi:10.1111/j.1365-294X.2010.04689.x. PubMed: 20618906.
30. Johannesson K, Panova M, Kemppainen P, André C, Rolán-Alvarez E et al. (2010) Repeated evolution of reproductive isolation in a marine snail: unveiling mechanisms of speciation. Philos Trans R Soc Lond B Biol Sci 365: 1735–1747. doi:10.1098/rstb.2009.0256. PubMed: 20439278.
31. Marshall DJ, Monro K, Bode M, Keough MJ, Swearer S (2010) Phenotype-environment mismatches reduce connectivity in the sea. Ecol Lett 13: 128–140. doi:10.1111/j.1461-0248.2009.01408.x. PubMed: 19968695.
32. Bird CE, Holland BS, Bowen BW, Toonen RJ (2011) Diversification of sympatric broadcast-spawning limpets (*Cellana* spp.) within the Hawaiian archipelago. Integr Comp Biol 51: E11–E11. PubMed: 21481050.
33. Sanford E, Kelly MW (2011) Local adaptation in marine invertebrates. In: CA CarlsonSJ Giovannoni. Annual Review of Marine Science 3: 509–535. doi:10.1146/annurev-marine-120709-142756
34. Ogden R, Thorpe RS (2002) Molecular evidence for ecological speciation in tropical habitats. Proc Natl Acad Sci U S A 99: 13612–13615. doi:10.1073/pnas.212248499. PubMed: 12370440.
35. Bierne N, Bonhomme F, David P (2003) Habitat preference and the marine-speciation paradox. Proc R Soc Lond B Biol Sci 270: 1399–1406. doi:10.1098/rspb.2003.2404. PubMed: 12965032.
36. Rocha LA, Robertson DR, Roman J, Bowen BW (2005) Ecological speciation in tropical reef fishes. Proc R Soc Lond B Biol Sci 272: 573–579. doi:10.1098/2004.3005. PubMed: 15817431.
37. Prada C, Hellberg ME (2013) Long prereproductive selection and divergence by depth in a Caribbean candelabrum coral. Proc Natl Acad Sci U S A 110: 3961–3966. doi:10.1073/pnas.1208931110. PubMed: 23359716.
38. Doebeli M, Dieckmann U (2003) Speciation along environmental gradients. Nature 421: 259–264. doi:10.1038/nature01274. PubMed: 12529641.
39. Irwin DE (2012) Local adaptation along smooth ecological gradients causes phylogeographic breaks and phenotypic clustering. Am Nat 180: 35–49. doi:10.1086/666002. PubMed: 22673649.
40. Nosil P, Vines TH, Funk DJ (2005) Perspective: Reproductive isolation caused by natural selection against immigrants from divergent habitats. Evolution 59: 705–719. doi:10.1554/04-428. PubMed: 15926683.
41. Schluter D (2009) Evidence for ecological speciation and its alternative. Science (Wash) 323: 737–741. doi:10.1126/science.1160006.
42. Keller I, Seehausen O (2012) Thermal adaptation and ecological speciation. Mol Ecol 21: 782–799. doi:10.1111/j.1365-294X.2011.05397.x. PubMed: 22182048.
43. Van Dover CL (2000) The ecology of deep-sea hydrothermal vents. Princeton, NJ: Princeton University Press. p. 1.
44. Vrijenhoek RC (2010) Genetic diversity and connectivity of deep-sea hydrothermal vent metapopulations. Mol Ecol 19: 4391–4411. doi:10.1111/j.1365-294X.2010.04789.x. PubMed: 20735735.
45. Bucklin A, Wilson RR Jr, Smith KL Jr (1987) Genetic differentiation of seamount and basin populations of the deep-sea amphipod *Eurythenes gryllus*. Deep Sea Research 34: 1795–1810. doi:10.1016/0198-0149(87)90054-9.
46. France SC, Kocher TD (1996) Geographic and bathymetric patterns of mitochondrial 16S rRNA sequence divergence among deepsea amphipods, *Eurythenes gryllus*. Mar Biol 126: 633–643. doi:10.1007/bf00351330.
47. Etter RJ, Rex MA, Chase MR, Quattro JM (2005) Population differentiation decreases with depth in deep-sea bivalves. Evolution 59: 1479–1491. doi:10.1554/04-538. PubMed: 16153033.
48. Zardus JD, Etter RJ, Chase MR, Rex MA, Boyle EE (2006) Bathymetric and geographic population structure in the pan-Atlantic deep-sea bivalve *Deminucula atacellana* (Schenck, 1939). Mol Ecol 15: 639–651. doi:10.1111/j.1365-294X.2005.02832.x. PubMed: 16499691.
49. Raupach MJ, Malyutina M, Brandt A, Wägele J-W (2007) Molecular data reveal a highly diverse species flock within the munnopsoid deep-sea isopod *Betamorpha fusiformis* (Barnard, 1920) (Crustacea : Isopoda : Asellota) in the Southern Ocean. Deep Sea Res II Topical Stud Oceanogr 54: 1820–1830. doi:10.1016/j.dsr2.2007.07.009.
50. Miller KJ, Rowden AA, Williams A, Häussermann V (2011) Out of their depth? isolated deep populations of the cosmopolitan coral *Desmophyllum dianthus* may be highly vulnerable to environmental change. PLOS ONE 6: e19004. doi:10.1371/journal.pone.0019004. PubMed: 21611159.
51. Etter RJ, Boyle EE, Glazier A, Jennings RM, Dutra E et al. (2011) Phylogeography of a pan-Atlantic abyssal protobranch bivalve: implications for evolution in the deep Atlantic. doi:10.1111/j.1365-294X.2010.04978.x.
52. White TA, Fotherby HA, Hoelzel AR (2011) Comparative assessment of population genetics and demographic history of two congeneric deep sea fish species living at different depths. Mar Ecol Prog Ser 434: 155–164. doi:10.3354/meps09207.
53. García-Merchán H, Robainas-Barcia A, Abelló P, Macpherson E, Palero F et al. (2012) Phylogeographic patterns of decapod crustaceans at the Atlantic-Mediterranean transition. Mol Phylogenet Evol 62: 664–672. doi:10.1016/j.ympev.2011.11.009. PubMed: 22138160.
54. Laakmann S, Auel H, Kochzius M (2012) Evolution in the deep sea: Biological traits, ecology and phylogenetics of pelagic copepods. Mol Phylogenet Evol 65: 535–546. doi:10.1016/j.ympev.2012.07.007. PubMed: 22842293.
55. Chase MR, Etter RJ, Rex MA, Quattro JM (1998) Bathymetric patterns of genetic variation in a deep-sea protobranch bivalve, *Deminucula atacellana*. Mar Biol 131: 301–308. doi:10.1007/s002270050323.
56. Quattro JM, Chase MR, Rex MA, Greig TW, Etter RJ (2001) Extreme mitochondrial DNA divergence within populations of the deep-sea gastropod *Frigidoalvania brychia*. Mar Biol 139: 1107–1113. doi:10.1007/s002270100662.
57. Etter RJ, Rex MA, Chase MC, Quattro JM (1999) A genetic dimension to deep-sea biodiversity. Deep Sea Res I Oceanogr Res Pap 46: 1095–1099. doi:10.1016/s0967-0637(98)00100-9.
58. Reveillaud J, Remerie T, van Soest R, Erpenbeck D, Cárdenas P et al. (2010) Species boundaries and phylogenetic relationships between Atlanto-Mediterranean shallow-water and deep-sea coral associated *Hexadella* species (Porifera, Ianthellidae). Mol Phylogenet Evol 56: 104–114. doi:10.1016/j.ympev.2010.03.034. PubMed: 20382244.
59. Schüller M (2011) Evidence for a role of bathymetry and emergence in speciation in the genus *Glycera* (Glyceridae, Polychaeta) from the deep Eastern Weddell Sea. Polar Biol 34: 549–564. doi:10.1007/s00300-010-0913-x.
60. Baird HP, Miller KJ, Stark JS (2011) Evidence of hidden biodiversity, ongoing speciation and diverse patterns of genetic structure in giant Antarctic amphipods. Mol Ecol 20: 3439–3454. doi:10.1111/j.1365-294X.2011.05173.x. PubMed: 21733028.
61. Gage JD, Tyler PA (1991) Deep-Sea Biology: A natural history of organisms at the deep-sea floor. Cambridge: Cambridge University Press. 504pp.
62. Carney RS (2005) Zonation of deep biota on continental margins. Oceanogr Mar Biol Annu Rev 43: 211–278.

63. Rex MA, Etter RJ (2010) Deep-Sea Biodiversity: Pattern and Scale. Cambridge, MA: Harvard University Press.
64. Levin LA, Sibuet M, Levin LA, Sibuet M (2012) Understanding Continental Margin Biodiversity: A New Imperative. In: CA CarlsonSJ Giovannoni. Annual Review of Marine, Vol 4. Science, Vol 4. Vol. 4: 79–112 doi:10.1146/annurev-marine-120709-142714. PubMed: 22457970.
65. Maddison WP (1997) Gene trees in species trees. Syst Biol 46: 523–536. doi:10.1093/sysbio/46.3.523.
66. Edwards SV, Beerli P (2000) Perspective: Gene divergence, population divergence, and the variance in coalescence time in phylogeographic studies. Evolution 54: 1839–1854. doi: 10.1554/0014-3820(2000)054[1839:pgdpda]2.0.co;2. PubMed: 11209764.
67. Pritchard JK, Stephens M, Donnelly P (2000) Inference of Population Structure Using Multilocus Genotype Data. Genetics 155: 945–959. PubMed: 10835412.
68. Felsenstein J (2006) Accuracy of coalescent likelihood estimates: Do we need more sites, more sequences, or more loci? Mol Biol Evol 23: 691–700. PubMed: 16364968.
69. Knowles LL, Carstens BC (2007) Delimiting species without monophyletic gene trees. Syst Biol 56: 887–895. doi: 10.1080/10635150701701091. PubMed: 18027282.
70. Toews DPL, Brelsford A (2012) The biogeography of mitochondrial and nuclear discordance in animals. Mol Ecol 21: 3907–3930. doi:10.1111/j.1365-294X.2012.05664.x. PubMed: 22738314.
71. Hessler RR, Sanders HL (1967) Faunal diversity in the deep-sea. Deep Sea Research 14: 65–78.
72. Jennings RM, Etter RJ (2011) Exon-primed, intron-crossing (EPIC) loci for five nuclear genes in deep-sea protobranch bivalves: primer design, PCR protocols and locus utility. Mol Ecol Resour 11: 1102–1112. doi: 10.1111/j.1755-0998.2011.03038.x. PubMed: 21689382.
73. Dmitriev DA, Rakitov RA (2008) Decoding of superimposed traces produced by direct sequencing of heterozygous indels. PLOS Comput Biol 4: e1000113. PubMed: 18654614.
74. Stephens M, Smith NJ, Donnelly P (2001) A new statistical method for haplotype reconstruction from population data. Am J Hum Genet 68: 978–989. doi:10.1086/319501. PubMed: 11254454.
75. Stephens M, Donnelly P (2003) A comparison of Bayesian methods for haplotype reconstruction from population genotype data. Am J Hum Genet 73: 1162–1169. doi:10.1086/379378. PubMed: 14574645.
76. Larkin MA, Blackshields G, Brown NP, Chenna R, McGettigan PA et al. (2007) Clustal W and Clustal X version 2.0. PubMed: 17846036
77. Conesa A, Götz S, García-Gómez JM, Terol J, Talón M et al. (2005) Blast2GO: a universal tool for annotation, visualization and analysis in functional genomics research. Bioinformatics 21: 3674–3676. doi: 10.1093/bioinformatics/bti610. PubMed: 16081474.
78. Keller O, Kollmar M, Stanke M, Waack S (2011) A novel hybrid gene prediction method employing protein multiple sequence alignments. Bioinformatics 27: 757–763. doi:10.1093/bioinformatics/btr010. PubMed: 21216780.
79. Zuker M (2003) Mfold web server for nucleic acid folding and hybridization prediction. Nucleic Acids Res 31: 3406–3415. doi: 10.1093/nar/gkg595. PubMed: 12824337.
80. Excoffier L, LISCHER HEL (2010) Arlequin suite ver 3.5: a new series of programs to perform population genetics analyses under Linux and Windows. Mol Ecol Resour 10: 564–567. doi:10.1111/j.1755-0998.2010.02847.x. PubMed: 21565059.
81. Li N, Stephens M (2003) Modeling linkage disequilibrium and identifying recombination hotspots using single-nucleotide polymorphism data. Genetics 165: 2213–2233. PubMed: 14704198.
82. Crawford DC, Bhangale T, Li N, Hellenthal G, Rieder MJ et al. (2004) Evidence for substantial fine-scale variation in recombination rates across the human genome. Nat Genet 36: 700–706. doi:10.1038/ng1376. PubMed: 15184900.
83. McDonald JH, Kreitman M (1991) Adaptive protein evolution at the Adh locus in Drosophila. Nature 351: 652–654. doi:10.1038/351652a0. PubMed: 1904993.
84. Falush D, Stephens M, Pritchard JK (2003) Inference of population structure using multilocus genotype data: linked loci and correlated allele frequencies. Genetics 155: 945–959. Available: http://www.genetics.org/content/164/4/1567.short. PubMed: 12930761.
85. Earl DA, vonHoldt BM (2011) STRUCTURE HARVESTER: a website and program for visualizing STRUCTURE output and implementing the Evanno method. Conserv Genet Resour 4: 359–361. doi:10.1007/s12686-011-9548-7.
86. Evanno G, Regnaut S, Goudet J (2005) Detecting the number of clusters of individuals using the software structure: a simulation study. Mol Ecol 14: 2611–2620. doi:10.1111/j.1365-294X.2005.02553.x. PubMed: 15969739.
87. Jakobsson M, Rosenberg NA (2007) CLUMPP: a cluster matching and permutation program for dealing with label switching and multimodality in analysis of population structure. Bioinformatics 23: 1801–1806. doi: 10.1093/bioinformatics/btm233. PubMed: 17485429.
88. Rosenberg NA (2004) distract: a program for the graphical display of population structure. Mol Ecol Notes 4: 137–138. doi:10.1046/j.1471-8286.2003.00566.x.
89. Clement M, Posada D, Crandall KA (2000) TCS: a program to estimate gene genealogies. Mol Ecol 9: 1657–1659. doi:10.1046/j.1365-294x.2000.01020.x. PubMed: 11050560.
90. Meirmans PG (2006) Using the AMOVA framework to estimate a standardized genetic differentiation measure. Evolution 60: 2399–2403. doi:10.1111/j.0014-3820.2006.tb01874.x. PubMed: 17236430.
91. Smouse PE, Long JC, Sokal RR (1986) Multiple regression and correlation extensions of the Mantel test of matrix correspondence. Syst Zool 35: 627–632. doi:10.2307/2413122.
92. Hey J, Nielsen R (2004) Multilocus methods for estimating population sizes, migration rates and divergence time, with applications to the divergence of Drosophila pseudoobscura and D. persimilis. Genetics 167: 747–760. doi:10.1534/genetics.103.024182. PubMed: 15238526.
93. Heled J, Drummond AJ (2008) Bayesian inference of population size history from multiple loci. Bmc. Evol Biol 8. doi: 10.1186/1471-2148-8-289.
94. Drummond AJ, Suchard MA, Xie D, Rambaut A (2012) Bayesian phylogenetics with BEAUti and the BEAST. p. 1.7. Mol Biol Evol 29: 1969–1973.
95. Heled J, Drummond AJ (2010) Bayesian inference of species trees from multilocus data. Mol Biol Evol 27: 570–580. doi:10.1093/molbev/msp274. PubMed: 19906793.
96. Zardus JD (2002) Protobranch bivalves. Adv Mar Biol 42: 1–65. doi: 10.1016/S0065-2881(02)42012-3. PubMed: 12094722.
97. Hudson RR, Turelli M (2003) Stochasticity overrules the "three-times rule": genetic drift, genetic draft, and coalescence times for nuclear loci versus mitochondrial dna. Evolution 57: 182–190. doi:10.1111/j.0014-3820.2003.tb00229.x. PubMed: 12643581.
98. Shaw KL (2002) Conflict between nuclear and mitochondrial DNA phylogenies of a recent species radiation: what mtDNA reveals and conceals about modes of speciation in Hawaiian crickets. Proc Natl Acad Sci U S A 99: 16122–16127. doi:10.1073/pnas.242585899. PubMed: 12451181.
99. Near TJ, Benard MF (2004) Rapid allopatric speciation in logperch darters (Percidae: *Percina*). Evolution 58: 2798–2808. doi:10.1111/j.0014-3820.2004.tb01631.x. PubMed: 15696757.
100. Johnson SB, Young CR, Jones WJ, Warén A, Vrijenhoek RC (2006) Migration, isolation, and speciation of hydrothermal vent limpets (Gastropoda ; Lepetodrilidae) across the Blanco Transform Fault. Biol Bull 210: 140–157. doi:10.2307/4134603. PubMed: 16641519.
101. Eytan RI, Hayes M, Arbour-Reily P, Miller M, Hellberg ME (2009) Nuclear sequences reveal mid-range isolation of an imperilled deep-water coral population. Mol Ecol 18: 2375–2389. doi:10.1111/j.1365-294X.2009.04202.x. PubMed: 19457199.
102. Maruyama T, Fuerst PA (1984) Population bottlenecks and nonequilibrium models in population genetics. I. allele numbers when populations evolve from zero variability. Genetics.
103. Excoffier L, Foll M, Petit RJ (2009) Genetic consequences of range expansions. Annu Rev Ecol 40: 481–501. doi:10.1146/annurev.ecolsys.39.110707.173414.
104. Bazin E, Glémin S, Galtier N (2006) Population size does not influence mitochondrial genetic diversity in animals. Science (Wash) 312: 570–572. doi:10.1126/science.1122033.
105. Galtier N, Nabholz B, Glémin S, Hurst GD (2009) Mitochondrial DNA as a marker of molecular diversity: a reappraisal - GALTIER -2009 - Molecular Ecology - Wiley Online Library. Mol Ecol 18: 4541–4550. doi: 10.1111/j.1365-294X.2009.04380.x. PubMed: 19821901.
106. Raupach MJ, Wägele JW (2006) Distinguishing cryptic species in Antarctic Asellota (Crustacea: Isopoda) - a preliminary study of mitochondrial DNA in *Acanthaspidia drygalskii*. Antarct Sci 18: 191–198. doi:10.1017/S0954102006000228.
107. Moura CJ, Harris DJ, Cunha MR, Rogers AD (2008) DNA bar coding reveals cryptic diversity in marine hydroids (Cnidaria, Hydrozoa) from coastal and deep-sea environments. Zool Scripta 37: 93–108. doi: 10.1111/j.1463-6409.2007.00312.x.
108. Scheltema RS, Williams IP (2009) Reproduction among protobranch bivalves of the family Nuculidae from sublittoral, bathyal, and abyssal depths off the New England coast of North America. Deep Sea Res II Topical Stud Oceanogr 56: 1835–1846. doi:10.1016/j.dsr2.2009.05.024.

109. Allen JA, Sanders HL (1996) The zoogeography, diversity and origin of the deep-sea protobranch bivalves of the Atlantic: The epilogue. Prog Oceanogr 38: 95–153. doi:10.1016/S0079-6611(96)00011-0.
110. Herrera S, Shank TM, Sánchez JA (2012) Spatial and temporal patterns of genetic variation in the widespread antitropical deep-sea coral *Paragorgia arborea*. Mol Ecol 21: 6053–6067. Available: http://onlinelibrary.wiley.com/doi/10.1111/mec.12074/full. doi:10.1111/mec.12074. PubMed: 23094936.
111. Cowart DA, Huang C, Arnaud-Haond S, Carney SL, Fisher CR et al. (2013) Restriction to large-scale gene flow vs. regional panmixia among cold seep *Escarpia* spp. (Polychaeta, Siboglinidae). Mol Ecol 22: 4147–4162. doi:10.1111/mec.12379. PubMed: 23879204.
112. Toole JM, Curry RG, Joyce TM, McCartney M, Peña-Molino B (2011) Transport of the North Atlantic Deep Western Boundary Current about 39°N, 70°W: 2004–2008. Deep Sea Res II Topical Stud Oceanogr 58: 1768–1780. doi:10.1016/j.dsr2.2010.10.058.
113. Bower A, Lozier S, Gary S (2011) Export of Labrador Sea Water from the subpolar North Atlantic: A Lagrangian perspective. Deep Sea Res II Topical Stud Oceanogr 58: 1798–1818. doi:10.1016/j.dsr2.2010.10.060.
114. Bower AS, Hendry RM, Amrhein DE, Lilly JM (2013) Direct observations of formation and propagation of subpolar eddies into the Subtropical North Atlantic. Deep Sea Res II Topical Stud Oceanogr 85: 15–41. doi:10.1016/j.dsr2.2012.07.029.
115. Lozier MS, Gary SF, Bower AS (2012) Simulated pathways of the overflow waters in the North Atlantic: Subpolar to subtropical export. Deep Sea Res II Topical Stud Oceanogr 85: 147–153. doi:10.1016/j.dsr2.2012.07.037.
116. Boyle EA, Keigwin LD (1982) Deep circulation of the North Atlantic over the last 200,000 years: geochemical evidence. Science (Wash) 218: 784–787. doi:10.1126/science.218.4574.784. PubMed: 17771034.
117. Keigwin LD, Pickart RS (1999) Slope Water Current over the Laurentian Fan on Interannual to Millennial Time Scales. Science (Wash) 286: 520–523. doi:10.1126/science.286.5439.520. PubMed: 10521345.
118. Somero GN (1992) Adaptations to high hydrostatic pressure. Annu Rev Physiol 54: 557–577. doi:10.1146/annurev.physiol.54.1.557. PubMed: 1314046.
119. Levin LA (2003) Oxygen minimum zone benthos: Adaptation and community response to hypoxia. Oceanography Mar Biol, Vol 41 41: 1–45.
120. Brown A, Thatje S (2011) Respiratory response of the deep-sea amphipod *Stephonyx biscayensis* indicates bathymetric range limitation by temperature and hydrostatic pressure. PLOS ONE 6: e28562. doi:10.1371/journal.pone.0028562. PubMed: 22174838.
121. Levin LA, Boesch DF, Covich A, Dahm C, Erséus C et al. (2001) The function of marine critical transition zones and the importance of sediment biodiversity. Ecosystems 4: 430–451. doi:10.1007/s10021-001-0021-4.
122. Rogers AD (2000) The role of the oceanic oxygen minima in generating biodiversity in the deep sea. Deep Sea Res II Topical Stud Oceanogr 47: 119–148. doi:10.1016/s0967-0645(99)00107-1.
123. Bongaerts P, Riginos C, Hay KB, van Oppen MJH, Hoegh-Guldberg O et al. (2011) Adaptive divergence in a scleractinian coral: physiological adaptation of *Seriatopora hystrix* to shallow and deep reef habitats. Bmc. Evol Biol 11. doi:10.1186/1471-2148-11-303.
124. Carlon DB, Budd AF (2002) Incipient speciation across a depth gradient in a scleractinian coral? Evolution 56: 2227–2242. doi:10.1554/0014-3820(2002)056[2227:isaadg]2.0.co;2. PubMed: 12487353.
125. Baco AR, Shank TM (2005) Population genetic structure of the Hawaiian precious coral *Corallium lauuense* (Octocorallia: Coralliidae) using microsatellites. In: A FreiwaldJM Roberts. Cold-Water Corals and Ecosystems; Erlangen Earth Conference Series. Berlin/Heidelberg: Springer-Verlag. pp. 663–678 doi:10.1007/3-540-27673-4_33.
126. Kirk NL, Andras JP, Harvell CD, Santos SR, Coffroth MA (2009) Population structure of *Symbiodinium* sp. associated with the common sea fan, *Gorgonia ventalina*, in the Florida Keys across distance, depth, and time. Mar Biol 156: 1609–1623. doi:10.1007/s00227-009-1196-z.
127. Cho W, Shank TM (2010) Incongruent patterns of genetic connectivity among four ophiuroid species with differing coral host specificity on North Atlantic seamounts. Mar Ecol 31: 121–143. doi:10.1111/j.1439-0485.2010.00395.x.
128. Costantini F, Rossi S, Pintus E, Cerrano C, Gili JM et al. (2011) Low connectivity and declining genetic variability along a depth gradient in *Corallium rubrum* populations. Coral Reefs 30: 991–1003. doi:10.1007/s00338-011-0771-1.
129. Baco AR, Cairns SD (2012) Comparing molecular variation to morphological species designations in the deep-sea coral *Narella* reveals new insights into seamount coral ranges. PLOS ONE, 7: e45555. PubMed: 23029093.
130. Moura CJ, Cunha MR, Porteiro FM, Yesson C, Rogers AD (2011) Evolution of Nemertesia hydroids (Cnidaria: Hydrozoa, Plumulariidae) from the shallow and deep waters of the NE Atlantic and western Mediterranean. Zool Scripta 41: 79–96. doi:10.1111/j.1463-6409.2011.00503.x.
131. Quattrini AM, Georgian SE; Byrnes L, Stevens A, Falco R et al. (2013) Niche divergence by deep-sea octocorals in the genus *Callogorgia* across the continental slope of the Gulf of Mexico. Mol Ecol. doi:10.1111/mec.12370.
132. van Oppen MJH, Bongaerts P, Underwood JN, Peplow LM, Cooper TF (2011) The role of deep reefs in shallow reef recovery: an assessment of vertical connectivity in a brooding coral from west and east Australia. Mol Ecol 20: 1647–1660. doi:10.1111/j.1365-294X.2011.05050.x. PubMed: 21410573.
133. Clague GE, Cheney KL, Goldizen AW, McCormick MI, Waldie PA et al. (2011) Long-term cleaner fish presence affects growth of a coral reef fish. Biol Lett 7: 863–865. Available: http://61.184.90.41:8000/rewriter/CNKI/http/qrak9qnx-krnbhdsxotakhrghmf9nqf/content/7/6/863.full. doi:10.1098/rsbl.2011.0458. PubMed: 21733872.
134. Castelin M, Puillandre N, Lozouet P, Sysoev A, de Forges BR et al. (2011) Molluskan species richness and endemism on New Caledonian seamounts: Are they enhanced compared to adjacent slopes? Deep Sea Res I Oceanogr Res Pap 58: 637–646. doi:10.1016/j.dsr.2011.03.008.
135. Ohsawa T, Ide Y (2008) Global patterns of genetic variation in plant species along vertical and horizontal gradients on mountains. Glob Ecol Biogeogr 17: 152–163. doi:10.1111/j.1466-8238.2007.00357.x.
136. Hensen I, Cierjacks A, Hirsch H, Kessler M, Romoleroux K et al. (2012) Historic and recent fragmentation coupled with altitude affect the genetic population structure of one of the world's highest tropical tree line species. Glob Ecol Biogeogr 21: 455–464. doi:10.1111/j.1466-8238.2011.00691.x.
137. Scott JW, Meyer SE, Merrill KR, Anderson VJ (2010) Local population differentiation in *Bromus tectorum* L. in relation to habitat-specific selection regimes. Evol Ecol 24: 1061–1080. doi:10.1007/s10682-010-9352-y.
138. Vega-Vela NE, Chacón Sánchez MI (2012) Genetic structure along an altitudinal gradient in Lippia origanoides, a promising aromatic plant species restricted to semiarid areas in northern South America. Ecol Evolution 2: 2669–2681. doi:10.1002/ece3.360. PubMed: 23170204.
139. Conover DO, Duffy TA, Hice LA (2009) The covariance between genetic and environmental influences across ecological gradients reassessing the evolutionary significance of countergradient and cogradient variation. In: CD SchlichtingTA Mousseau. Year in Evolutionary Biology 2009. Vol. 1168. pp. 100–129. doi:10.1111/j.1749-6632.2009.04575.x
140. Ehinger M, Fontanillas P, Petit E, Perrin N (2002) Mitochondrial DNA variation along an altitudinal gradient in the greater white-toothed shrew, *Crocidura russula*. Mol Ecol 11: 939–945. doi:10.1046/j.1365-294X.2002.01487.x. PubMed: 11975709.
141. Giordano AR, Ridenhour BJ, Storfer A (2007) The influence of altitude and topography on genetic structure in the long-toed salamander (*Ambystoma macrodactulym*). Mol Ecol 16: 1625–1637. doi:10.1111/j.1365-294X.2006.03223.x. PubMed: 17402978.
142. Oromi N, Richter-Boix A, Sanuy D, Fibla J (2012) Genetic variability in geographic populations of the natterjack toad (*Bufo calamita*). Ecol Evolution 2: 2018–2026. doi:10.1002/ece3.323. PubMed: 22957202.
143. Byars SG, Parsons Y, Hoffmann AA (2009) Effect of altitude on the genetic structure of an Alpine grass, *Poa hiemata*. Ann Bot 103: 885–899. doi:10.1093/aob/mcp018. PubMed: 19208670.
144. Dubey S, Shine R (2010) Restricted dispersal and genetic diversity in populations of an endangered montane lizard (*Eulamprus leuraensis*, Scincidae). Mol Ecol 19: 886–897. doi:10.1111/j.1365-294X.2010.04539.x. PubMed: 20149087.
145. Barker JSF, Frydenberg J, Sarup P, Loeschcke V (2011) Altitudinal and seasonal variation in microsatellite allele frequencies of *Drosophila buzzatii*. J Evol Biol 24: 430–439. doi:10.1111/j.1420-9101.2010.02180.x. PubMed: 21091575.
146. Keller I, Taverna A, Seehausen O (2011) Evidence of neutral and adaptive genetic divergence between European trout populations sampled along altitudinal gradients. Mol Ecol 20: 1888–1904. doi:10.1111/j.1365-294X.2011.05067.x. PubMed: 21418113.
147. Bulgarella M, Peters JL, Kopuchian C, Valqui T, Wilson RE et al. (2012) Multilocus coalescent analysis of haemoglobin differentiation between low- and high-altitude populations of crested ducks (*Lophonetta specularioides*). Mol Ecol 21: 350–368. doi:10.1111/j.1365-294X.2011.05400.x. PubMed: 22151704.

148. Cheviron ZA, Brumfield RT (2009) Migration-selection balance and local adaptation of mitochondrial haplotypes in rufous-collared sparrows (*Zonotrichia capensis*) along an elevational gradient. Evolution 63: 1593–1605. doi:10.1111/j.1558-5646.2009.00644.x. PubMed: 19187247.
149. Snyder LRG, Hayes JP, Chappell MA (1988) Alpha-chain hemoglobin polymorphisms are correlated with altitude in the deer mouse, *Peromyscus maniculatus*. Evolution 42: 689–697. doi: 10.2307/2408860.
150. Burgess MD, Nicoll MAC, Jones CG, Norris K (2011) Multiple environmental gradients affect spatial variation in the productivity of a tropical bird population. J Anim Ecol 80: 688–695. doi:10.1111/j.1365-2656.2011.01816.x. PubMed: 21463301.
151. Danovaro R, Gambi C, Dell'Anno A, Corinaldesi C, Fraschetti S et al. (2008) Exponential decline of deep-sea ecosystem functioning linked to benthic biodiversity loss. Curr Biol 18: 1–8. doi:10.1016/j.cub.2007.11.056. PubMed: 18164201.
152. Danovaro R, Umani SF, Pusceddu A (2009) Climate change and the potential spreading of marine mucilage and microbial pathogens in the Mediterranean Sea. PLOS ONE 4: e7006. doi:10.1371/journal.pone.0007006. PubMed: 19759910.
153. Glover AG, Gooday AJ, Bailey DM, Billett DSM, Chevaldonné P et al. (2010) Temporal change in deep-sea benthic ecosystems: A review of the evidence from recent time-series studies. Adv Mar Biol 58: 1–95. doi:10.1016/B978-0-12-381015-1.00001-0. PubMed: 20959156.
154. Ramirez-Llodra E, Tyler PA, Baker MC, Bergstad OA, Clark MR et al. (2011) Man and the last great wilderness: human impact on the deep sea. PLOS ONE 6: e22588. doi:10.1371/journal.pone.0022588. PubMed: 21829635.
155. Harris PT, Whiteway T (2009) High seas marine protected areas: Benthic environmental conservation priorities from a GIS analysis of global ocean biophysical data. Ocean & Coastal Management 52: 22–38.
156. Clark MR, Watling L, Rowden AA, Guinotte JM (2011) A global seamount classification to aid the scientific design of marine protected area networks. Ocean & Coastal Management 54: 19–36.